



California State University **Chico**

EECE 653 Software Defined Radio  
Lab 1 Amplitude Modulation (AM) Modulator

Yolanda D. Reyes

September 24, 2024

# Table of Contents

|                                                                |             |
|----------------------------------------------------------------|-------------|
| 1. Introduction                                                |             |
| 1.1 Digital Communication Systems .....                        | pp. 1 - 5   |
| 2. Calculations                                                |             |
| 2.1 Common Emitter with Carrier Signal: Large Signal .....     | pp. 5 - 9   |
| 2.2 Common Emitter with Carrier Signal: Small Signal .....     | pp. 9 - 13  |
| 2.3 Tank Circuit .....                                         | pp. 1 - 14  |
| 3. Simulations                                                 |             |
| 3.1 MATLAB .....                                               | pp. 14 - 18 |
| 3.2 LtSPICE .....                                              | pp. 18 - 19 |
| 4. Experimental Results                                        |             |
| 4.1 Common Emitter with Carrier Signal .....                   | pp. 19 - 21 |
| 4.2 Common Emitter with Carrier and Message Signals .....      | pp. 21 - 22 |
| 4.3 Common Emitter with Message Signals and Tank Circuit ..... | pp. 22 - 23 |
| 4.4 Tank Circuit Tuning with Capacitors .....                  | pp. 24 - 27 |
| 5. Results and Conclusion                                      |             |
| 5.1 Results .....                                              | pp. 27      |
| 5.2 Discussion .....                                           | pp. 27 - 29 |
| 5.3 Conclusion .....                                           | pp. 29      |
| 6. Datasheets                                                  |             |
| NPN Transistor Datasheet .....                                 | pp. 30 - 35 |
| 7. References .....                                            | pp. 36 - 37 |

# 1. Introduction

## 1.1. Digital Communication Systems

Traditional radio frequency (RF) communication systems can trace their origin back to 1886 when Heinrich Hertz built the first apparatus for generating and detecting radio waves [1]. One of the first widely utilized RF communication systems developed in the 1890s is morse code which was transmitted using radiotelegraphy [2,3]. Early RF communication systems required specific hardware to generate, modulate, transmit and receive RF signals. Because of this hardware dependency pre-software defined radio (SDR) systems were not flexible and only capable of operating under the restrictions set by the hardware. Over the past 130+ years many standards and protocols such as the International Telecommunication Union (ITU-T) standard for audio copanding, G.711, the audio codec protocol G.722, and the Internet Protocol Suite (TCP/IP) have been widely adopted and are still in use today [4,5,6]. The rapidly evolving telecommunication landscape meant that with each new protocol or standard existing systems needed their hardware redesigned to stay in compliance with newest conventions. Because of the development and improvement of electronics components such as the integrated circuit (IC), analog-to-digital converters (ADC), and digital-to-analog converters (DAC) a transition away from the hardware restricted traditional RF communication systems towards flexible software defined radio (SDR) systems could be realized [7,8,9,10].

SDR systems employ several improved techniques such as digital signal processing (DSP), direct digital synthesis (DDS), and signal modulation. Before DSP traditional RF communication systems performed filtering, modulation, demodulation and amplification via analog circuits using resistors, capacitors, inductors, and operational amplifiers tuned to specific behaviors. DSP improved these areas of RF systems by enabling the hardware to stay fixed, while providing flexibility by using software programming to implement variability of these key features. Modulation, the act of combining a carrier signal with a message signal for transmission, demodulation, the act of extracting the original message signal from the carrier signal after receiving, filtering, the enhancing and attenuating of specific frequencies of interest and amplification, when implemented in SDR systems, use Discrete Fourier Transform (DFT), Fast Fourier Transform (FFT), scalar multiplication and convolution algorithms to achieve flexibility with the fixed hardware. Generating precise and stable frequency wave forms also improved to enable SDR.

Analog signal synthesis in pre-SDR FM communication systems employed analog components such as Voltage-Controlled Oscillators (VCOs), and Phase-Locked Loops (PLLs) to achieve precise frequency waveform generation. While these components are still used in the hardware of SDR systems there is no need to create VCOs or PLLs for every possible waveform of interest. By implementing a phase accumulator, which increments by one phase step at each clock cycle, and calculating step size, the SDR system is capable of

generating precise frequencies. The limiting factor in this type of waveform generation shifts from hardware based limitations to frequency resolution which is dependent on the number of bits in the phase accumulator, and the DAC which determines how finely the output waveform's amplitude can be represented. Major advantages with SDR over traditional FM communication systems includes the ability for rapid tuning, quick frequency adjustments "hopping", and lower phase noise. These advantages enable complex, multi-frequency and phase coherent waveforms to be dynamically generated which also provide an SDR system with multi-functionality and multi-mode capabilities. Being able to generate a wide range of frequency waveforms in software is a crucial task in modern communication systems. Signal modulation methods are equally important to modern communication systems and benefit greatly when implemented in an SDR paradigm.

Traditional RF communication systems require dedicated hardware designs to provide access to modulation schemes, seen in Fig. 1, such as Amplitude Modulation (AM), and Frequency Modulation (FM). However in an SDR system software provides the flexibility of switching between schemes which is essential in multi-mode communication devices such as smartphones which use protocols such as Global System for Mobile Communications (GSM), Code-Division Multiple Access (CDMA) and Long Term Evolution (LTE).

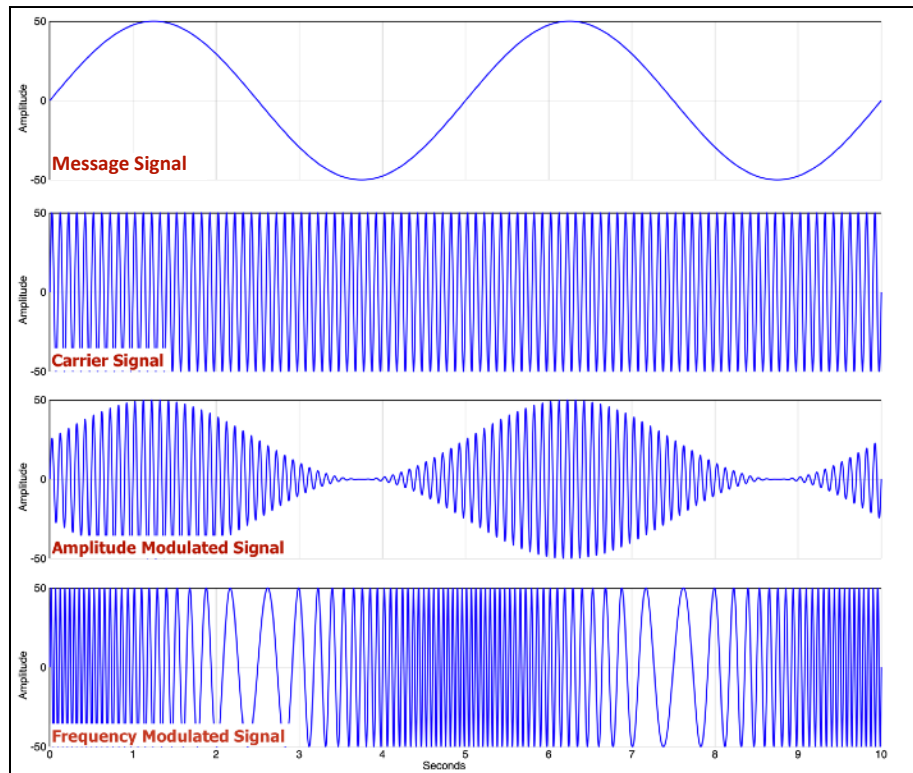


**Fig. 1** Plots of a message signal,  $m(t)$ , carrier signal,  $c(t)$ , with both the Amplitude Modulation (AM) scheme, and Frequency Modulation (FM) scheme applied resulting in output signal  $y(t)$ . These two popular modulation methods are used to transmit encoded data with a carrier signal. By analyzing the modulation effects  $m(t)$  has on  $c(t)$  data is extracted from the transmitted signal. Image © 2022 Brian Pickle [11].

In early telecommunication systems the AM scheme was implemented using modulator tubes and a signal mixer, in modern non-SDR systems the analog components required to achieve the AM scheme include an oscillator to produce the carrier signal, a modulator to produce the data signal and an operational amplifier. The benefit of utilizing an SDR system to implement the AM scheme is in the leveraging of algorithms to digitally combine the message signal and the carrier signal in the modulator block, showcased in Fig. 2. It is important to note that with the AM scheme noise greatly affects the amplitude, which is the feature that carries the information. Because of this susceptibility to data loss due to noise, the FM scheme was developed.

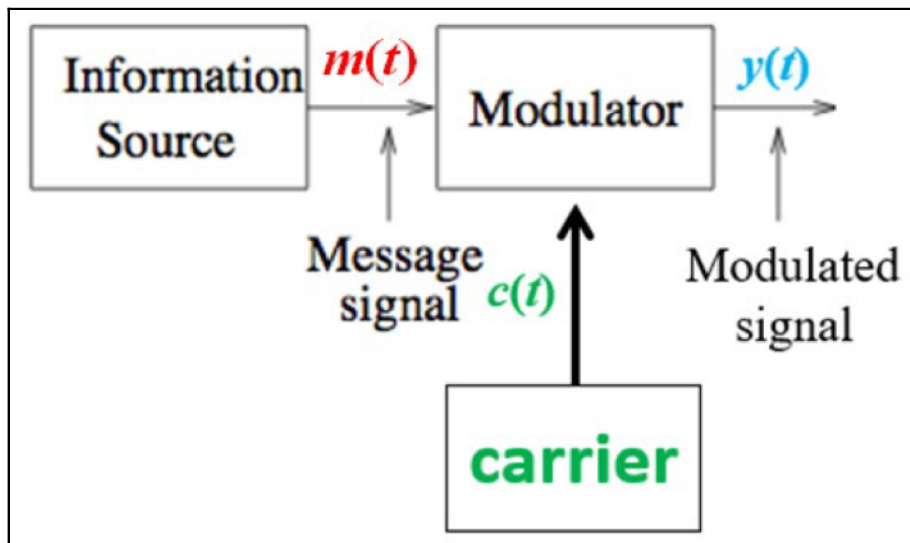


**Fig. 2** Diagram of message signal  $m(t)$ , carrier signal,  $c(t)$ , entering the modulator/signal mixer block in a RF communication system. The modulation process must be efficient to ensure the transmitted signal is strong enough with a low signal-to-noise ratio so that it can be received over long distances with data integrity maintained. Analog components in modern modulator blocks include transistors which replaced vacuum tubes capable of handling the high power required for broadcasting. Image © 2024 Dr. Ghang-Ho Lee.

In Fig. 3 a typical SDR transmitter system is presented [12]. The Data Source block is where the information originates which can be sound, video, text, etc. The Source Encoder block compresses/encodes, the data which will enable a reduction in transmission

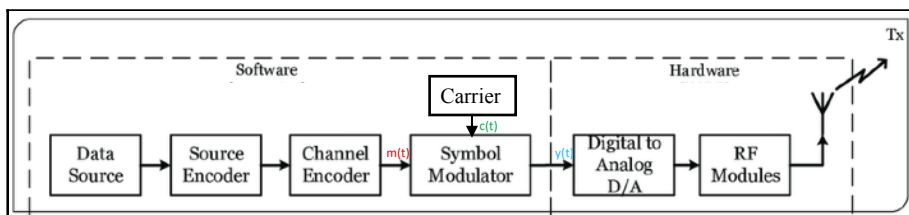


**Fig. 3** Block diagram of Software Defined Radio (SDR) transmitter with software elements on the left, and hardware components on the right. By utilizing the flexibility of an SDR implemented communication system are capable of dynamically adapting through software updates instead of hardware changes, and can also be multi-functional operating according to many standards/protocols. Image © 2019 Hussein Kwasme & Sabit Ekin [12].

bandwidth requirements without significant loss of information. Some common compression algorithms include MPEG and H.264. The Channel Encoder is vital in error detection and correction before modulation, DAC, and ultimately transmission by improving the resiliency of data during transmission over noisy channels. Depending on the SDR system implementation the convolutional algorithm may be deployed in the Channel Encoder to support data integrity regardless of errors during transmission because it is easy to implement in software. The Symbol Modulator utilizes software techniques that map bits to symbols which indicate changes in amplitude, frequency or phase depending on the transmission modulation scheme selected.

Lab 1 work is focused on the Symbol Modulator block, in Fig. 2 & 3. For Lab 1 it is assumed that the message signal,  $m(t)$ , has already been processed by the Source and Channel Encoders presented in Fig. 3. A key concept explored in Lab 1 is the tuning of the modulator block by varying capacitor  $C_3$  in the tank circuit presented in Fig. 4. In Fig. 5 the tank circuit is connected to  $V_{cc}$  and the collector port of NPN BJT  $Q_1$  this implementation determines how much voltage and power is delivered to  $R_L$ . Considering the next circuit

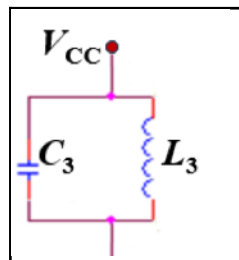


**Fig. 4** Diagram of tank circuit from Lab 1. The tank circuit resonates at specific frequencies, depending on the value of  $C_3$  and  $L_3$ , which directly affect signal filtering and transmission frequency. Image © 2024 Dr. Ghang-Ho Lee.

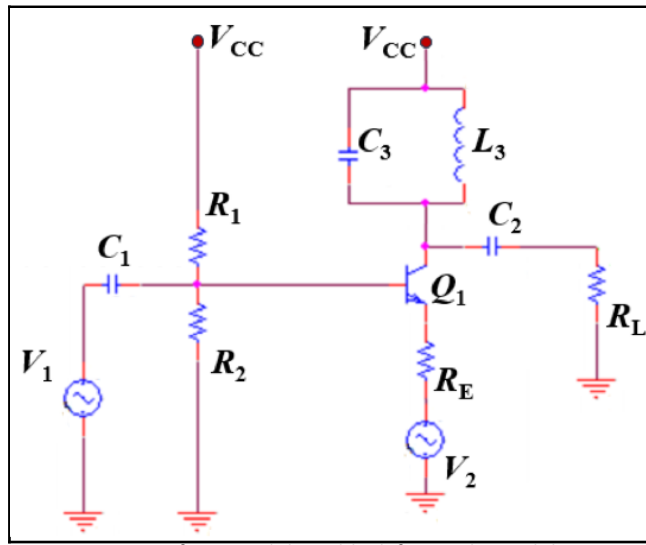


**Fig. 5** Diagram of AM modulator block from Lab 1. While you can vary inductor  $L_3$  or capacitor  $C_3$ , in Lab 1 the experiments were conducted by keeping  $L_3$  fixed and varying  $C_3$ . Image © 2024 Dr. Ghang-Ho Lee.

modules in the AM transmitter would be the DAC, and an antenna it is important that the tank circuit pass clear signals close to the main carrier frequency of our  $c(t)$  signal so that the transmitter achieves high signal purity and reduces interferences from unwanted frequencies. The DAC is responsible for converting the modulated signal,  $y(t)$ , back to an analog signal before transmission. If the tank circuit does not resonate close to the frequency of  $c(t)$  the DAC may incorrectly convert the digital signal resulting in dataloss within the transmitted signal. In addition to stabilizing the frequency of the AM transmitter oscillations, properly tuning the tank circuit is crucial for maximum power transfer, and

impedance matching which directly impact the quality of the signal transmitted. By effectively transferring power to the antenna the signal can efficiently propagate into the air positively impacting the range and strength of the transmitted signal. If a design doesn't ensure most of the power generated reaches the antenna, it is highly likely power will reflect back into the transmitter and dissipate as heat in the circuit. Another important feature to note about an SDR FM communication system, that is directly related to the tank circuit operation, is the highly sought after multi-mode and multi-frequency communication capabilities found in modern commercial and tactical military communication systems. By utilizing L<sub>3</sub> or C<sub>3</sub> components with variability the system is able to provide this functionality to the user.

## 2. Calculations

### 2.1. Common Emitter with Carrier Signal: Large Signal

To implement the Lab 1 AM transmitter we start off performing calculations on an NPN BJT in common emitter configuration, see Fig 6. The first part of the analysis for Lab 1 involves calculations to determine the forward active operating region of the base circuit. Several important values to properly perform this analysis came from the datasheet for the 2N3904 NPN BJT, see page 31, including V<sub>BE\_SAT</sub>, which indicate the turn on voltage from the

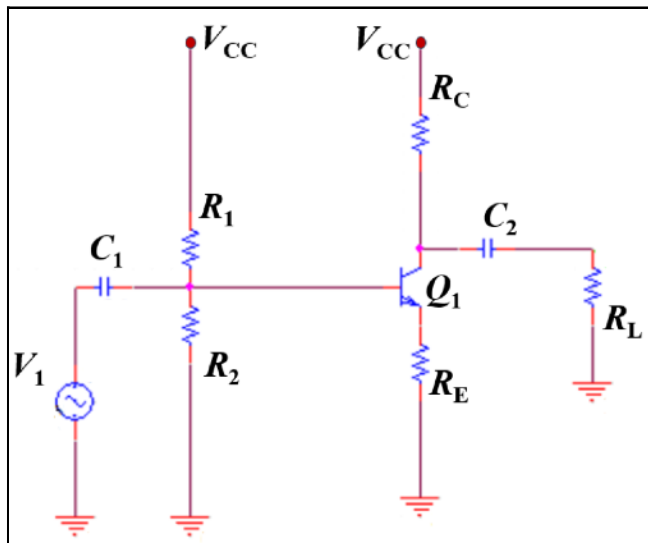
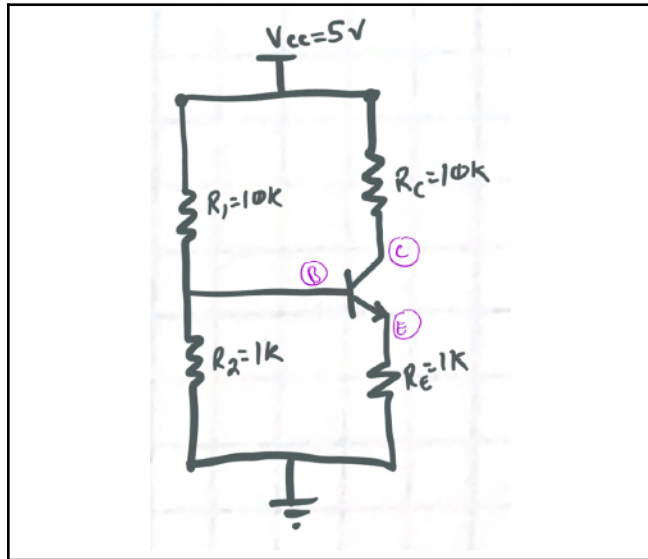


Fig. 6 Diagram of common emitter circuit with carrier signal,  $c(t)$  represented by  $V_1$ . Image © 2024 Dr. Ghang-Ho Lee.

base to emitter ports of Q<sub>1</sub>, as well as  $\beta$ . In large signal analysis of the circuit presented in Fig. 6 we first acknowledge that C<sub>1</sub> and C<sub>2</sub> are considered to be open circuits. Because of this re-drawing the circuit diagram is helpful, see Fig. 7, to perform further analysis such as determining the Thevenin voltage and resistance. To determine the Thevenin voltage and resistance the following equations were used:

$$V_{th} = V_{cc} * R_2 / (R_1 + R_2) \quad (1)$$

$$R_{th} = (R_1 * R_2) / (R_1 + R_2) \quad (2)$$



**Fig. 7** Diagram of large signal equivalent circuit with values provided in Lab 1 documentation as well as base, collector and emitter ports clearly labeled. Image © 2024 Yolanda Reyes.

Calculating equations (1) & (2) it was determined that  $V_{th}$  is 454.55 [mV] and the  $R_{th}$  is 909.09 [ $\Omega$ ]. The next step in large signal analysis is to once again re-draw the circuit, Fig 8., so that Kirchhoff's Voltage Law (KVL) can be used in the Base-Emitter and Collector-Emitter loops.

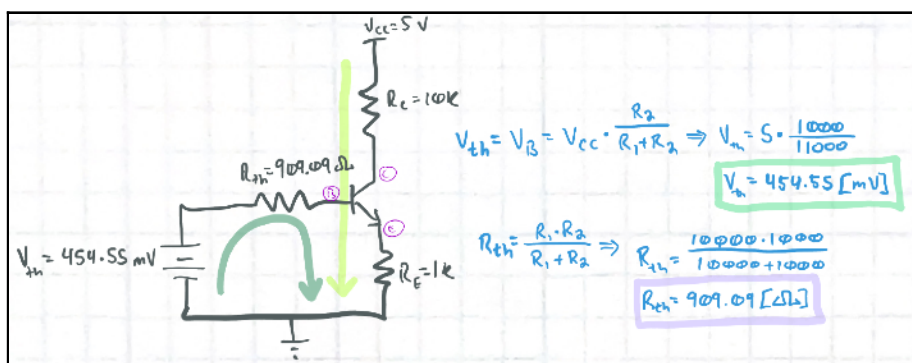


**Fig. 8** Diagram of Thevenin equivalent circuit with calculated values for  $V_{th}$  and  $R_{th}$  in addition to the KVL loops labeled that we will use to calculate current values  $I_B$ ,  $I_C$ , and  $I_E$ . Image © 2024 Yolanda Reyes.

Analyzing the circuit in Fig. 8 it was determined that the equations for the Base-Emitter and Collector-Emitter KVL loops are as follows:

$$B-E \text{ Loop: } V_{th} - [I_B * R_{th}] - V_{BE\_ON} - [I_E * R_E] = 0 \quad (3)$$

$$C-E \text{ Loop: } V_{cc} - [I_C * R_C] - V_{CE\_SAT} - [I_E * R_E] = 0 \quad (4)$$

At this point in the calculations the values of  $I_B$ ,  $I_C$ , or  $I_E$  are still unknown. This is when Ohm's Law can be used to determine the value of  $I_B$ :

$$I_B = (V_{th} - V_{BE\_ON}) / (R_{th} + (1 + \beta) * R_E) \quad (5)$$

Performing the calculation for equation (5) it is determined that the value of  $I_B$  is  $-1.94$  [ $\mu A$ ], and now enough information is available to proceed with calculating, see Fig. 9., the values of  $I_C$  and  $I_E$  using the equations:

$$I_C = \beta * I_B \quad (6)$$

$$I_E \approx I_C \quad (7)$$

|                                                                                                                                                                                                                                                                                                                                                                             |                                                                                                                                                                                                                                                                                                                                                  |
|-----------------------------------------------------------------------------------------------------------------------------------------------------------------------------------------------------------------------------------------------------------------------------------------------------------------------------------------------------------------------------|--------------------------------------------------------------------------------------------------------------------------------------------------------------------------------------------------------------------------------------------------------------------------------------------------------------------------------------------------|
| $V_{BE\_min}$<br>$I_B = \frac{454.55 \times 10^3 - 650 \times 10^{-3}}{909.09 + (1 + 100) \cdot 1000}$<br>$I_B = \frac{-195.46 \times 10^{-3}}{100909.09}$<br>$I_B = -1.94 \times 10^{-6} [A]$<br>$\therefore I_C = \beta \cdot I_B$<br>$I_C = 1000 \cdot -1.94 \times 10^{-6} [A]$<br>$I_C = -193.69 \times 10^{-6} [A]$<br>$I_E \approx I_C = -193.69 \times 10^{-6} [A]$ | $V_{BE\_max}$<br>$I_B = \frac{454.55 \times 10^3 - 850 \times 10^{-3}}{909.09 + (1 + 100) \cdot 1000}$<br>$I_B = \frac{-395.46 \times 10^{-3}}{100909.09}$<br>$I_B = -3.92 \times 10^{-6} [A]$<br>$\therefore I_C = 1000 \cdot -3.92 \times 10^{-6} [A]$<br>$I_C = -392.89 \times 10^{-6} [A]$<br>$I_E \approx I_C = -392.89 \times 10^{-6} [A]$ |
|-----------------------------------------------------------------------------------------------------------------------------------------------------------------------------------------------------------------------------------------------------------------------------------------------------------------------------------------------------------------------------|--------------------------------------------------------------------------------------------------------------------------------------------------------------------------------------------------------------------------------------------------------------------------------------------------------------------------------------------------|

Fig. 9 Calculation for current values  $I_B$ ,  $I_C$ , and  $I_E$ . Using the information provided in the 2N3904 NPN BJT datasheet found at page 31 there is a range of turn on voltages possible. This was taken into account and so presented here are the lower and upper limits for current through  $I_B$ ,  $I_C$ , and  $I_E$ . Image © 2024 Yolanda Reyes.

Using these calculated values for  $I_B$ ,  $I_C$ , and  $I_E$  all values for the variables in equations (3) & (4) are now known and can be confirmed using KVL, see Fig. 10.

|                                                                                                                                                                                                                                                                                                                                                                                                                                                                                                                                                                                          |                                                                                                                                                                                                                                                                                                                                                     |
|------------------------------------------------------------------------------------------------------------------------------------------------------------------------------------------------------------------------------------------------------------------------------------------------------------------------------------------------------------------------------------------------------------------------------------------------------------------------------------------------------------------------------------------------------------------------------------------|-----------------------------------------------------------------------------------------------------------------------------------------------------------------------------------------------------------------------------------------------------------------------------------------------------------------------------------------------------|
| $KVL \text{ B-E:}$<br>$V_{th} - I_B \cdot R_{th} - I_E \cdot R_E = 0$<br>$[454.55 \times 10^3] - [I_B \cdot 909.09] - [I_E \cdot 1000] = 0$<br>$[454.55 \times 10^3] - [I_B \cdot 909.09] - [(100) \cdot I_B \cdot 1000] = 0$<br><br>$V_{BE\_min}$<br>$[454.55 \times 10^3] - [-1.94 \times 10^{-6} \cdot 909.09] - [(1 + 100) \cdot -1.94 \times 10^{-6} \cdot 1000] = 0$<br>$[454.55 \times 10^3] - [-1.96 \times 10^{-3}] - [-195.44 \times 10^{-6} \cdot 1000] = 0$<br>$[454.55 \times 10^3] - [-1.96 \times 10^{-3}] - [-195.44 \times 10^{-3}] = 0$<br>$652.25 \times 10^{-3} = 0$ | $V_{BE\_max}$<br>$[454.55 \times 10^3] - [-3.92 \times 10^{-6} \cdot 909.09] - [(1 + 100) \cdot -3.92 \times 10^{-6} \cdot 1000] = 0$<br>$[454.55 \times 10^3] - [-3.56 \times 10^{-3}] - [-395.92 \times 10^{-6} \cdot 1000] = 0$<br>$[454.55 \times 10^3] - [-3.56 \times 10^{-3}] - [-395.92 \times 10^{-3}] = 0$<br>$854.03 \times 10^{-3} = 0$ |
|------------------------------------------------------------------------------------------------------------------------------------------------------------------------------------------------------------------------------------------------------------------------------------------------------------------------------------------------------------------------------------------------------------------------------------------------------------------------------------------------------------------------------------------------------------------------------------------|-----------------------------------------------------------------------------------------------------------------------------------------------------------------------------------------------------------------------------------------------------------------------------------------------------------------------------------------------------|

Fig. 10 Calculation for KVL Loop from Base-Emitter using calculated current values  $I_B$ ,  $I_C$ , and  $I_E$  from Fig. 9. The initial results found indicate error. Image © 2024 Yolanda Reyes.

Due to the errors found during the first attempt at calculating the large signal values presented in Fig. 10., analysis of this circuit required re-calculating equations (1) - (7). Performing calculations in Fig. 8 - 10 it was determined that  $R_2$  with a value of 1 [ $k\Omega$ ], would not be sufficient to put  $Q_1$  into forward active mode. Since the voltage divider circuit consisting of  $R_1$  and  $R_2$  is only providing 454.55 [mV] to the base port of  $Q_1$  the value of  $R_2$  needed to be increased. For the second round of calculations  $R_2$  with a value of 2 [ $k\Omega$ ] was selected and equations (1) - (7) were re-calculated, see Fig. 11.

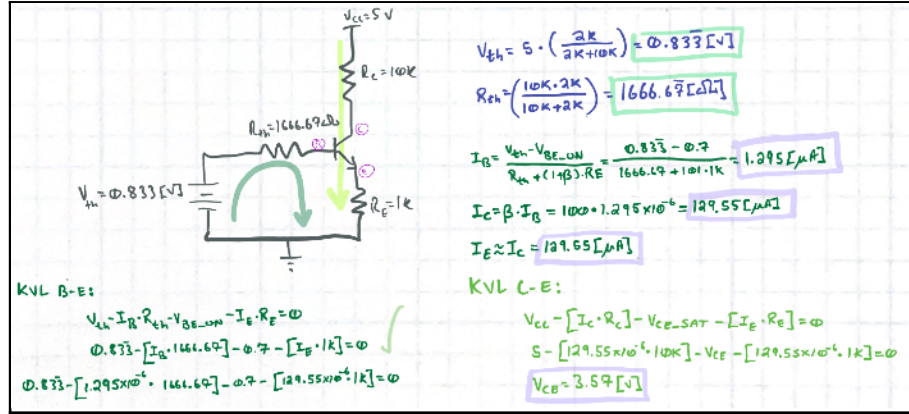


**Fig. 11** Re-calculating  $V_{th}$ ,  $R_{th}$ ,  $I_B$ ,  $I_C$ ,  $I_E$ , KVL Loops from Base-Emitter, and from Collector-Emitter. In this iteration of calculations the voltage divider circuit is sending enough voltage to  $Q_1$ 's base port for the circuit to be in forward active mode. Unlike the  $V_{BE\_ON}$  max/min calculations performed in **Fig. 9 - 10** here the average  $V_{BE\_ON}$  voltage, 0.7 [V], was used.  
Image © 2024 Yolanda Reyes.

After the second round of calculations the large signal analysis yielded favorable values for these variables of interest:

$$\begin{aligned} V_{th} &\approx 0.833 \text{ [V]} \\ R_{th} &\approx 1667 \text{ [\Omega]} \\ I_B &\approx 1.29 \text{ [\mu A]} \\ I_C &\approx 129.55 \text{ [\mu A]} \\ I_E &\approx 129.55 \text{ [\mu A]} \\ V_{CE} &= 3.57 \text{ [V]} \end{aligned}$$

With the voltage divider providing enough voltage to the base port of  $Q_1$  the next step in calculations performed aims to confirm the circuit is in forward active mode using Ohm's Law:

$$V = I * R \quad (8)$$

These calculations, showcased in Fig. 12., yielded  $V_B = 0.831 \text{ [V]}$ ,  $V_C = 3.705 \text{ [V]}$ , and  $V_E = 0.130 \text{ [V]}$  and confirmed that  $Q_1$  would be operating in forward active mode.

|                                                     |                                               |
|-----------------------------------------------------|-----------------------------------------------|
| $V_B = V_{Th} - [I_B \cdot R_{Th}]$                 | $V_E = I_E \cdot R_E$                         |
| $V_B = 0.833 - [1.29 \times 10^{-6} \cdot 1666.67]$ | $V_E = 129.55 \times 10^{-6} \cdot 1k$        |
| $V_B = 0.831 [V]$                                   | $V_E = 0.130 [V]$                             |
| $V_C = V_{cc} - [I_c \cdot R_C]$                    | $V_C = 5 - [129.55 \times 10^{-6} \cdot 10k]$ |
| $V_C = 3.705 [V]$                                   | $V_B = 0.831 [V]$                             |
|                                                     | $V_E = 0.130 [V]$                             |
|                                                     |                                               |

Fig. 12 Calculating  $V_B$ ,  $V_C$ , and  $V_E$  confirms the circuit will operate in forward active mode.  
Image © 2024 Yolanda Reyes.

## 2.2. Common Emitter with Carrier Signal: Small Signal

Using the values calculated in section 2.1 there is enough information to move onto the small signal analysis portion of Lab 1 calculations. In the small signal analysis independent voltages, such as  $V_{cc}$ , will be considered as a short circuit to GND, and  $C_1$  shorts to  $V_1$ , see Fig. 6. When performing small signal analysis several equations are used to determine the values of input resistance,  $r_\pi$ , transconductance,  $gm$ , and output resistance,  $r_o$ :

$$r_\pi = V_{Thermal} / I_B \quad (9)$$

$$gm = I_c / V_{Thermal} \quad (10)$$

$$r_o = V_A / I_C \quad (11)$$

It is important to note that in this situation  $r_o$ , is considered to be an open circuit due to the fact that the Early voltage,  $V_A$ , which quantifies the Early effect is  $\infty$ . This is because with an operating tank circuit at the collector port of  $Q_1$  there should be no significant variation in the voltage at the collector, the characteristic described by the Early effect. Input resistance represents,  $r_\pi$ , the input impedance of the transistor from the base port's perspective and determines how much the transistor loads the circuit driving it. Another important characteristic of the input resistance is that it is considered beneficial if equation (9) returns a very high value since this indicates signal integrity will be preserved and will prevent significant voltage drop across the base port of  $Q_1$ . The transconductance,  $gm$ , equation quantifies the capability of the transistor  $Q_1$  to convert variations from input voltage,  $V_1$  also known as the carrier signal  $c(t)$ , across the base-emitter junction into output current changes through the collector-emitter portion of the circuit. A higher  $gm$  value implies greater amplification ability in the design. As seen in Fig. 13 the value calculated for  $r_\pi$  is  $20,077 [\Omega]$ , and the value of  $gm$  is  $0.00498 [1/\Omega]$ .

Handwritten calculations for small signal variables:

$$r_{\pi} = \frac{26k \times 10^{-3}}{1.295 \times 10^{-6}} \therefore r_{\pi} = 20077.32 [\Omega]$$

$$g_m = \frac{129.55k \times 10^{-6}}{26k \times 10^{-3}} \therefore g_m = 0.00498 [\delta] \text{ or } \left[ \frac{1}{26} \right]$$

$$r_o = \frac{\infty}{I_c} = \infty \text{ "OPEN"}$$

**Fig. 13** The small signal variable calculations using values obtained during large signal analysis and 2N3904 NPN BJT datasheet on page 31. Image © 2024 Yolanda Reyes.

The next step in the small circuit analysis requires that the circuit presented in Fig. 6. be re-drawn to the small signal equivalent circuit, as presented in Fig. 14.

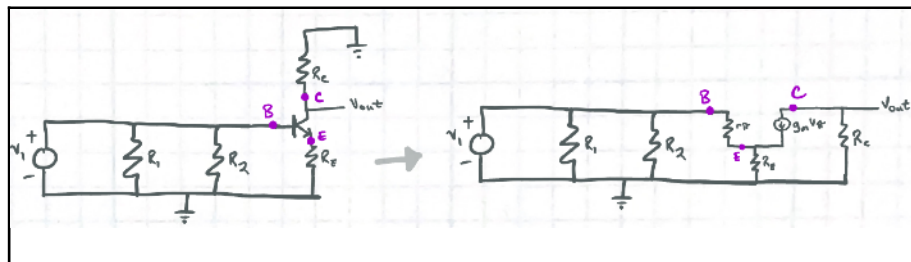


**Fig. 14** The small signal equivalent circuit has several notable features when compared to the circuit presented in **Fig. 6.**, such as  $C_1$  is now a short circuit directly to  $V_1$ , and  $V_{cc}$  is a short circuit directly to GND. Image © 2024 Yolanda Reyes.

With the circuit re-drawn it is easier to analyze using test voltage and currents. In small signal analysis input and output resistances as well as voltage gain and current is calculated. As with previous steps it is helpful to re-draw the circuit, labeling variables of interest, and then using equation (8) and KVL. In Fig. 15. input resistance,  $R_i$ , is determined to take on the form of:

(12)

$$R_i = R_1 \parallel R_2 \parallel R_{eq\_Base}$$

Using Ohm's Law we determine that the equivalent resistance to the base port of  $Q_1$  is  $R_{eq\_Base}$  which takes on the form of:

(13)

$$R_{eq\_Base} = V_{test} / I_{test}$$

Performing KVL from across the Base-Emitter ports of  $Q_1$ , an equation in the form of (13) can be derived. Since all values on one side are known the final calculation for input resistance is performed and returns a value of 121.0779 [ $k\Omega$ ].

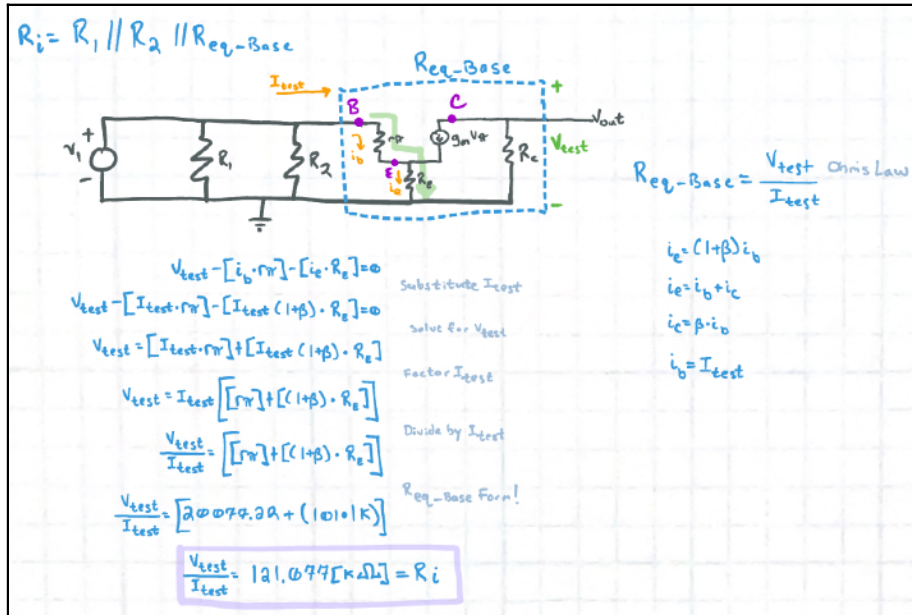


Fig. 15 Calculating the input resistance requires the use of a test voltage and current. Image © 2024 Yolanda Reyes.

The same workflow is followed to analyze the output resistance,  $R_o$ , by first re-drawing the circuit in Fig. 14, it is determined, in Fig. 16., that  $R_{eq\_Collector}$  takes on the form of:

$$R_{eq\_Base} = V_{test} / I_{test} = R_C \quad (14)$$

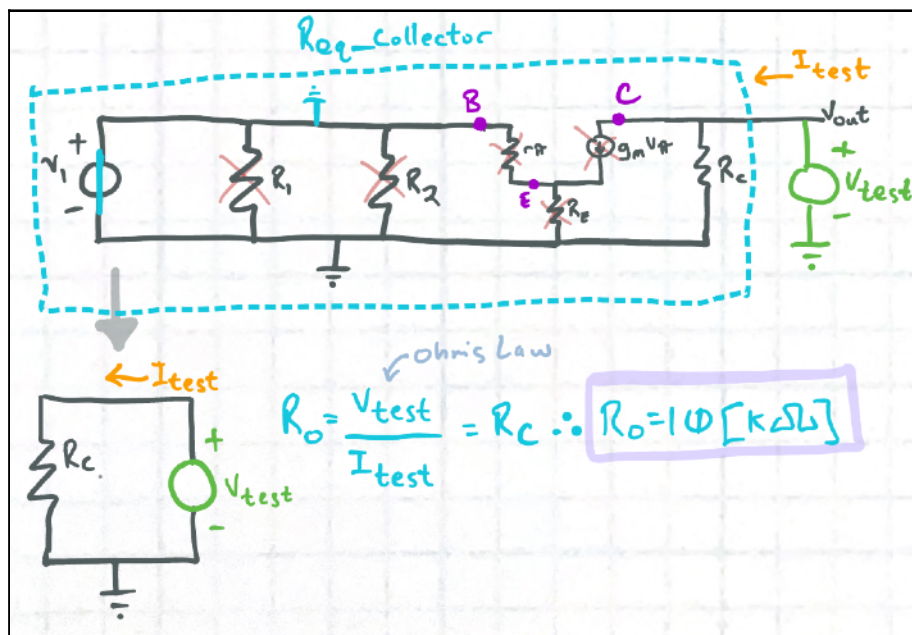


Fig. 16 Calculating the output resistance also requires the use of a test voltage and current. Because the independent voltage source is considered a short in the small signal analysis the equivalent circuit becomes  $R_C$  which is already known and equal to  $10[\text{k}\Omega]$ . Image © 2024 Yolanda Reyes.

The final step in the small signal analysis is to determine the voltage gain,  $A_V$ , which is defined by the equation:

$$A_V = V_o/V_i \quad (15)$$

Determining the values of voltage in,  $V_i$ , and voltage out,  $V_o$ , is clear when the circuit is re-drawn to just consider these two variables, as seen in Fig. 17.

The calculation for the KVL loop through the Base-Emitter portion of the circuit takes on the form of:

$$V_i - [i_b * r_\pi] - [i_e * R_E] = 0 \quad (16)$$

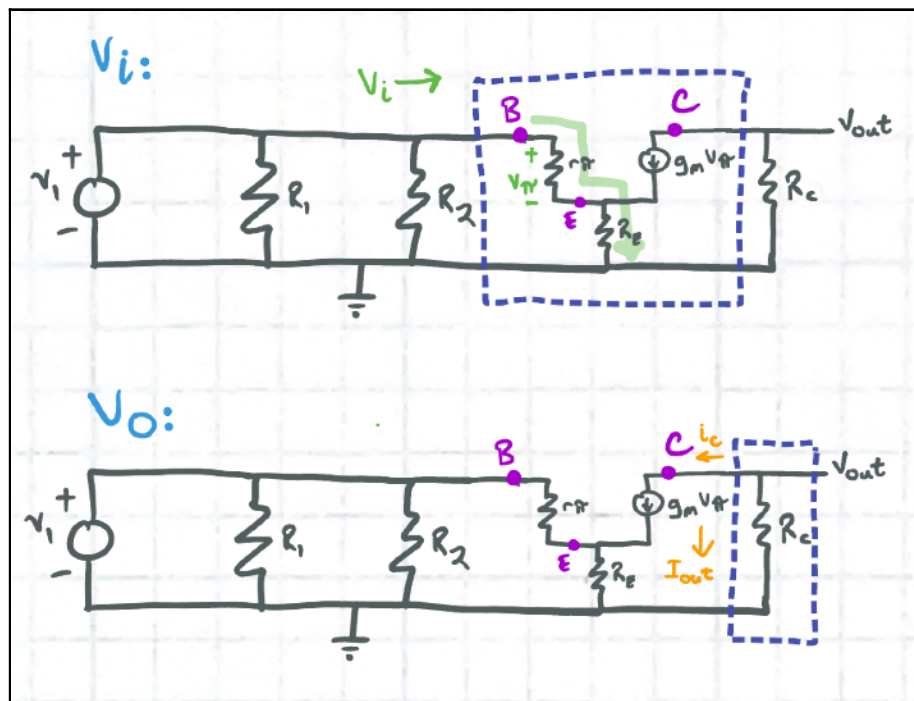


**Fig. 17** Calculating the values of  $V_i$  and  $V_o$  will provide enough information to determine the overall voltage gain of the circuit originally presented in **Fig. 6**. This information is obtained by utilizing KVL through the Base-Emitter loop and through  $R_C$ . It is important to note that  $I_{out} = -i_c = gm * V_\pi$ . Image © 2024 Yolanda Reyes.

The calculations for  $V_i$  and  $V_o$  are presented in Fig. 18, and result in a voltage gain,  $A_V$ , of 8.259, and a current gain of  $\approx 100 \times 10^{-6}$ . Some important relationships to take note of concerning calculating voltage gain,  $A_V$ , include that if the value of  $R_C$  increases so will  $A_V$ . However if the value of  $R_E$  increases  $A_V$  will decrease. The values of  $gm * r_\pi = \beta$ , and  $i_c = gm V_\pi$ .

$V_i - [i_b \cdot r_{\pi}] - [i_e \cdot R_E] = 0$   
 $i_b = \frac{V_i}{r_{\pi} + (1 + \beta) \cdot R_E}$  Ohm's Law  
 $V_{\pi} = \frac{V_i}{r_{\pi} + (1 + \beta) \cdot R_E} \cdot r_{\pi}$  Ohm's Law  
 $A_V = 8.259 [V]$   
 $A_I = \frac{I_o}{I_i} = \frac{i_b}{i_c}$   
 $A_I = \frac{2}{20049.22 + [100 \cdot 1K]}$   
 $A_I = 1.000015 [A]$   
 $V_o = I_{out} \cdot R_o$  Ohm's Law  
 $V_o = -i_c \cdot R_o$  Equivalent Current  
 $V_o = (g_m \cdot V_{\pi}) \cdot R_o$  Equivalent Current  
 $V_o = -[g_m \left( \frac{V_i}{r_{\pi} + (1 + \beta) \cdot R_E} \right) \cdot r_{\pi}] \cdot R_o$  Substitute  $V_{\pi}$   
 $\frac{V_o}{V_i} = -\left[ \frac{g_m \cdot r_{\pi}}{r_{\pi} + (1 + \beta) \cdot R_E} \right] \cdot R_o$  GAIN Form!  
 $\frac{V_o}{V_i} = -\left[ \frac{\beta \cdot R_o}{r_{\pi} + (1 + \beta) \cdot R_E} \right]$  Substitute  $\beta \cdot R_o$   
 $\frac{V_o}{V_i} = -\frac{100 \cdot 10K}{20049.22 + (100 \cdot 1K)}$  Solve for GAIN "Av"

Fig. 18 Calculating the values of  $V_i$  and  $V_o$  will provide enough information to determine the overall voltage gain of the circuit originally presented in Fig. 6. This information is obtained by utilizing KVL through the Base-Emitter loop which is labeled in Fig. 17. and through  $R_C$ . It is important to note that  $I_{out} = -i_c = g_m \cdot V_{\pi}$ . Image © 2024 Yolanda Reyes.

### 2.3. Tank Circuit

The tank circuit presented in Fig. 4 & 5. naturally oscillates at a specific frequency, called the resonance frequency, when capacitive and inductive reactances are equal to each other. In Lab 1 the tank circuit is implemented in parallel and the behavior of this circuit is assessed to be similar to an open circuit. This open circuit behavior is leveraged in SDR applications to implement signal selection and filtering as was conducted in the AM Transmitter Lab 1 experiments. To determine the resonance frequency of the tank circuit the following equation is used:

$$F_o = (1) / (2\pi * (L \cdot C)^{0.5}) \quad (17)$$

Where  $L$  is the value of the inductor in the circuit and  $C$  is the value of the capacitor. With variable capacitors and inductors the tank circuit is capable of resonating in a wide range of frequencies. When the capacitor value varies finer control over the exact resonance frequency is gained, whereas a change in the inductor will offer broader shifts in frequency. The quality or Q-factor is modeled by the equation:

$$Q = R(L/C)^{0.5} \quad (18)$$

The Q-factor describes how underdamped an oscillator is meaning how quickly the oscillations will move toward equilibrium. This implies that, assuming the resistance in the circuit is also fixed, a change in the inductor value will significantly impact the Q-factor. For this reason in Lab 1 the inductor was kept at a fixed value of 1 [mH], while three capacitors with values of 0.01 [ $\mu F$ ], 0.22 [ $\mu F$ ], and 0.47 [ $\mu F$ ] were implemented during the experiment. Lab 1 also utilized ceramic capacitors because as the capacitor is charged we need both terminals to enable charging on both sides. With an electrolytic capacitor the leads are polarized allowing charging to only take place on one side.

Fig. 19. showcases the calculations performed to determine the tank circuit resonance frequency for the three capacitors selected and also mathematically proves why maximum

current flows towards the emitter port of Q<sub>1</sub> by finding total impedance of the tank circuit implemented in Lab 1.

|                                                                                                                                                                                                                                                                                                                                                                                                                                                                                                                                                                                                                                                                                                                                                                                                                                                                                                                                                                                                                                                                                                                                                                                                                                                                                                                                                                                                                                                                                                                                                                                                                                                                   |  |                                                                                            |
|-------------------------------------------------------------------------------------------------------------------------------------------------------------------------------------------------------------------------------------------------------------------------------------------------------------------------------------------------------------------------------------------------------------------------------------------------------------------------------------------------------------------------------------------------------------------------------------------------------------------------------------------------------------------------------------------------------------------------------------------------------------------------------------------------------------------------------------------------------------------------------------------------------------------------------------------------------------------------------------------------------------------------------------------------------------------------------------------------------------------------------------------------------------------------------------------------------------------------------------------------------------------------------------------------------------------------------------------------------------------------------------------------------------------------------------------------------------------------------------------------------------------------------------------------------------------------------------------------------------------------------------------------------------------|--|--------------------------------------------------------------------------------------------|
|  <b>CHICO STATE</b><br><b>ENGINEERING</b>                                                                                                                                                                                                                                                                                                                                                                                                                                                                                                                                                                                                                                                                                                                                                                                                                                                                                                                                                                                                                                                                                                                                                                                                                                                                                                                                                                                                                                                                                                                                        |  | Name <u>Yolanda Reyes</u><br>Subject <u>EECE 653 Lab 2 Theory</u><br>Date <u>9-23-2024</u> |
| <p>Tank Circuit Resonance: <math>Z_L = Z_C</math></p> $Z_L = j\omega L = 2\pi f L$ $Z_C = \frac{1}{j\omega C} = \frac{1}{2\pi f C}$ $2\pi f L = \frac{1}{2\pi f C}$ $2\pi f^2 L = \frac{1}{2\pi C}$ $\frac{f^2}{2\pi^2} = \frac{1}{2\pi C} \Rightarrow f^2 = \frac{1}{2\pi^2 C} + \frac{1}{2\pi L}$ $f = \sqrt{\frac{1}{2\pi^2 C} + \frac{1}{2\pi L}}$ $f = \frac{1}{2\pi \sqrt{LC}}$ <p>Multiply f</p> <p>Solve for f</p> <p>Simplify</p> <p><math>C_3 = 0.01 \mu F</math>:</p> $f = \frac{1}{2\pi \sqrt{0.01 \times 10^{-6} \mu + 1/m}}$ <p><math>\therefore</math> Tank Circuit Resonance Frequency = 50.329 [kHz]</p> <p><math>C_3 = 0.02 \mu F</math>:</p> $f = \frac{1}{2\pi \sqrt{0.02 \times 10^{-6} \mu + 1/m}}$ <p><math>\therefore</math> Tank Circuit Resonance Frequency = 1.0473 [kHz]</p> <p><math>C_3 = 0.044 \mu F</math>:</p> $f = \frac{1}{2\pi \sqrt{0.044 \times 10^{-6} \mu + 1/m}}$ <p><math>\therefore</math> Tank Circuit Resonance Frequency = 734.124 [Hz]</p> <p><math>C_3</math> Impedance: <math>Z_C = \frac{1}{2\pi f C}</math></p> $Z_C = 2\pi (50.329 \times 10^3) \times 0.01 \times 10^{-6}$ $Z_C = 316.229 [\Omega]$ <p><math>L_3</math> Impedance:</p> $Z_L = 2\pi f L$ $Z_L = 2\pi (50.329 \times 10^3) \times (1 \times 10^{-3})$ $Z_L = 316.229 [\Omega]$ <p>Total Impedance of Tank Circuit:</p> $Z_{parallel} = \frac{1}{\frac{1}{Z_L} + \frac{1}{Z_C}}$ $Z_{parallel} = \left( \frac{1}{316.229 \times 10^3} \right) + \left( \frac{1}{316.229 - 10^3} \right)$ <p><math>\therefore</math> Undefined since division by zero.<br/>exhibits <math>\infty</math> impedance ensuring all current goes to emitter port.</p> |  |                                                                                            |

Fig. 19 Calculating the resonance frequency for three capacitors utilized during the experimental portion of Lab 1.  
Image © 2024 Yolanda Reyes.

### 3. Simulations

#### 3.1. MATLAB

To run MATLAB simulations for spectrum analyzer output the message signal, m(t), and carrier signal, c(t), need to be represented in the time-domain. The first step is to utilize the trigonometry identity to generalize the output signal y(t):

$$\cos(A) * \cos(B) = 1/2 [\cos(A-B) + \cos(A+B)] \quad (19)$$

In MATLAB our goal was to simulate the expected output, y(t), over time as well as the frequency-domain spectrum analyzer output for different message signal frequencies. With equation (16) calculated the Fourier Transform of this equation is required, to complete this process and analyze output in the frequency domain:

$$\cos(2\pi f_m t) \Rightarrow (1/2) [\delta[2\pi(f-f_m)t] + \delta[2\pi(f+f_m)t]] \quad (20)$$



Name Yolanda Reyes  
 Subject EECE 653 Lab 1 Theory  
 Date 9-9-2024

2. Recall WiFi router and the values from previous lectures. The operating frequency for message signal,  $m(t)$ , was 300 [Mbps or MHz]. The operating frequency for carrier signal,  $c(t)$ , was 2.4 [GHz]. We will use smaller values to build AM modulator and to simulate this situation due to limitations on the discrete parts we are using.

Assume "message signal",  $m(t)$ , is a **sine wave** with amplitude of 0.5 [Vp-p] and frequency of 300 [Hz]. Assume "carrier signal",  $c(t)$ , is a **sine wave** with amplitude of 2 [Vp-p] and frequency 50 [kHz].

- a. [Theory] Find time-domain representation of  $m(t)$ ,  $c(t)$ , and modulated signal,  $y(t)$  (using trigonometric identity, similar to what we went through in lecture).

$$m(t) = 300 \text{ Mbps or MHz} \text{ operating } f$$

$$A_{m(t)} = 0.5 \text{ [Vp-p]}$$

$$f_{m(t)} = 300 \text{ [Hz]}$$

$$m(t) = A_m \cdot \cos(2\pi f_m t)$$

$$m(t) = 0.5 \cdot \cos(2\pi 300t)$$

$$m(t) = 0.5 \sin(2\pi 300t - \frac{\pi}{2})$$

$$\text{AM Formula: } y(t) = A_c [1 + k \cdot m(t)] \cdot \cos(2\pi f_c t)$$

$$y(t) = 2 [1 + 0.25 \cdot 0.5 \cos(2\pi 300t) \cdot \cos(2\pi 50t)]$$

$$y(t) = 2 [1.125 \cos(2\pi 300t) \cdot \cos(2\pi 50t)] \quad \text{Cos}(A) \cdot \text{Cos}(B) = \frac{1}{2} [\text{Cos}(A-B) + \text{Cos}(A+B)] \text{ to generalize signal}$$

2a.

$$m(t) \cdot c(t) = \frac{1}{2} [\cos(2\pi 300t - 2\pi 50t) + \cos(2\pi 300t + 2\pi 50t)]$$

$$\frac{1}{2} \cdot \frac{1}{2} [\delta[2\pi(f - (50k - 300))] + \delta[2\pi(f - (50k + 300))] + \frac{1}{2} \cdot \frac{1}{2} [\delta[2\pi(f - (50k + 300))] + \delta[2\pi(f + (50k + 300))]] \xrightarrow{\text{FT:}} \frac{1}{2} [\delta[2\pi(f - f_m)t] + \delta[2\pi(f + f_m)t]] \text{ to look @ signal}$$

$$\frac{1}{4} [\delta[2\pi(f - 49.7\pi)] + \delta[2\pi(f - 50.3\pi)] + \frac{1}{4} [\delta[2\pi(f - 50.3\pi)] + \delta[2\pi(f + 49.7\pi)]]$$

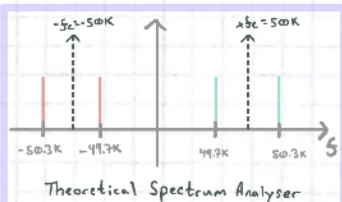


**Fig. 20** Calculating the time-domain equation for the message signal  $m(t)$ , and carrier signal,  $c(t)$ . With the resulting equation taking the Fourier Transform of this equation allows for the theoretical spectrum analyzer to be assessed prior to conducting the experiment in Lab 1. Image © 2024 Yolanda Reyes.

Even though the theoretical spectrum analyzer traces, see Fig. 20., included the negative frequency peaks at -49.7 [kHz] and -50.3 [kHz] these peaks were not presented in the MATLAB simulations, see Fig. 22 - 24, nor in our experiment bench-top tool Scopy interface showcasing FFT plots, see Fig. 34, 37 & 38. In the output the sidebands represent the actual message signal,  $m(t)$ , data. The carrier signal,  $c(t)$ , carries the lower frequency  $m(t)$  signal so it can be transmitted efficiently over a higher frequency band. Transmitting over a higher frequency helps reduce noise and interference which greatly affect lower frequency bands. By analyzing the sidebands presented as peaks in the MATLAB simulations the bandwidth of the transmission is also indicated. Utilizing the foundational code provided by Dr. Lee as a starting point and including the equations for  $m(t)$  operating at 300 [Hz], and  $c(t)$  operating at 50 [kHz], the simulation for the AM transmitter spectrum can be run, see Fig. 21.

```

Editor - /Users/scholar/Desktop/Chico State/Fall 2024/EECE 653/Lab 1/FFT_Ref_01.m
FFT_Ref_01.m  Prep_Lab_01_a_MATLAB_HW.m  +
3 T = 10; % defining time RANGE
4 Ts = 0.00002; % defining time STEP SIZE [seconds]
5 tn = -T/2:Ts:T/2; % defining time array -5 to 5 [seconds]
6
7 F = 1/Ts; % defining frequency RANGE from time STEP SIZE
8 Fs = 1/T; % defining frequency STEP SIZE from frequency RANGE
9 fn = 0:Fs:F; % defining frequency array
10 fn_2 = fn-F/2; % defining frequency array (zero at center)
11
12 mt = 0.5*cos(2*pi*300*t); % Message signal Am = 0.5 [Vp-p], f = 300 [Hz]
13 ct = 2*cos(2*pi*50000*t); % Carrier signal Ac = 2 [Vp-p], f = 50[kHz]
14 yt = mt.*ct; % Modulated signal, mt content towards ct freq. with sidebands @+- 49.7 & 50.3 [kHz]
15 %xt = 10*sin(2*pi*10*t); % time domain signal
16
17 Ys = fft(yt); % Perform FFT to find frequency domain signal
18 L_Ys = length(Ys); % Measuring length of Ys to perform AMPLITUDE NORMALIZATION
19
20 Ys_2 = fftshift(Ys)./(L_Ys./2); % FFTSHIFT and AMPLITUDE NORMALIZATION, makes plot symmetrical about 0 [Hz]
21
22 figure(1)
23
24 % ***** y(t) vs Time *****
25 subplot(2,1,1), plot(tn, yt, 'LineWidth', 2, 'Color', [0.9290 0.6940 0.1250]), grid on; xlabel('Time [sec]'); ylabel('y(t)');
26 xlim([-5e-6, 5e-6]);
27 ylim([-2, 2]);
28
29 % *****|Y(f)| vs Frequency *****
30 subplot(2,1,2), plot(fn_2, abs(Ys_2), 'LineWidth', 2, 'Color', [0.04470 0.7410]), grid on; xlabel('Freq [kHz]'); ylabel('|Y(f)|');
31 xlim([49e3, 51e3]);
32 ylim([-0.01, 1]);
33
34
35 %
36 % The amplitude spectrum of |Y(f)| in the blue plot confirms the results
37 % obtained in the theory portion of the Theory, Simulation homework
38 % assigned, problem part 2. What is different from the expected theoretical
39 % plot drawn versus what the MATLAB plot shows is that we are not observing
40 % the negative frequency sidebands peaking at -49.7 [kHz] or -50.3[kHz] due to
41 % the x-axis limits. The sidebands carry the actual message signal mt while
42 % the carrier signal "carries" the lower frequency mt signal to be transmitted
43 % efficiently over a higher frequency band which helps reduce noise and
44 % interference which are present in lower frequency bands. The sidebands
45 % help us determine the bandwidth of the signal allowing us to find the
46 % frequency spectrum the modulated signal, yt, occupies.
47 %
48 %
49

```

**Fig. 21** MATLAB simulation source code for  $m(t)$  with  $0.5 \text{ [V}_{\text{p-p}]\text{]}$  and frequency of  $300 \text{ [Hz]}$ , and  $c(t)$  with  $2 \text{ [V}_{\text{p-p}]\text{]}$  and frequency of  $50 \text{ [kHz]}$ . In line 12, the 300 took on values of 500, and 900 to simulate different operating frequencies for the message signal  $m(t)$ . Image © 2024 Yolanda Reyes.

The resulting plots from the code presented in Fig. 21 include the simulated output signal  $y(t)$  over time and expected spectrum analyzer peaks, see Fig. 22. In the time domain the amplitude of  $y(t)$  changes depending on the phase of  $m(t)$ . When  $m(t)$  is operating at

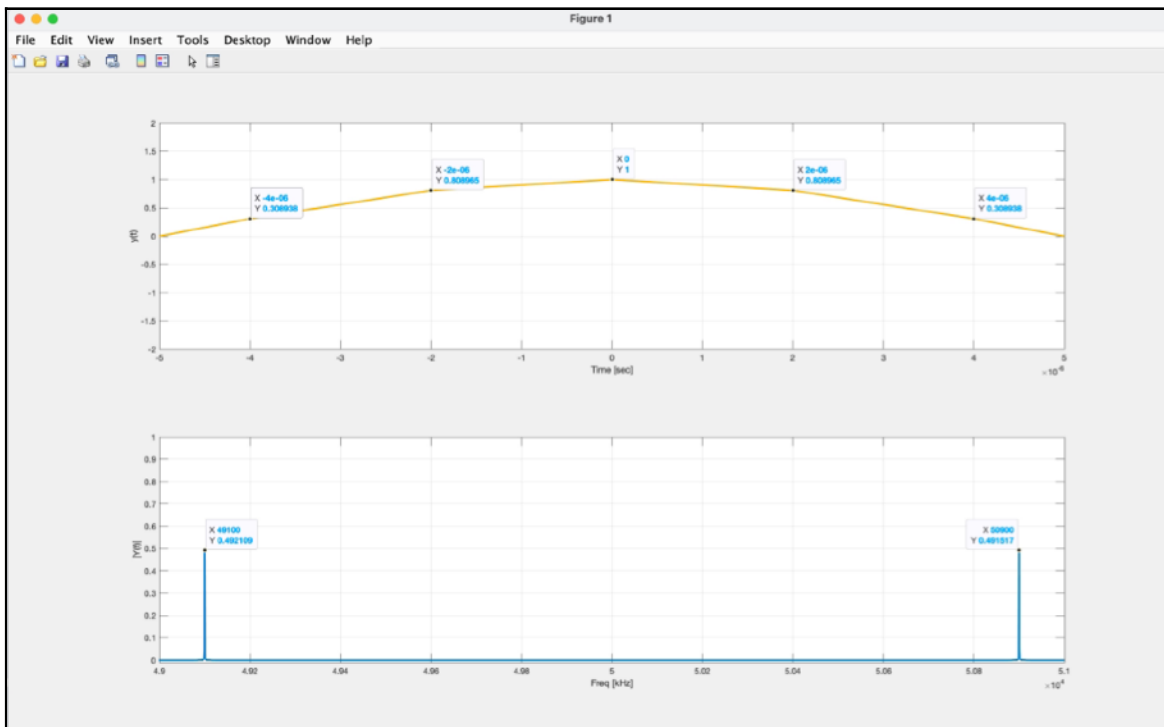


**Fig. 22** MATLAB plots from source code presented in Fig. 21. for  $m(t)$  with  $0.5 \text{ [V}_{\text{p-p}]\text{]}$  and frequency of  $300 \text{ [Hz]}$ , and  $c(t)$  with  $2 \text{ [V}_{\text{p-p}]\text{}}$  and frequency of  $50 \text{ [kHz]}$ . This simulation confirmed results form the theoretical calculations presented int Fig. 20. Image © 2024 Yolanda Reyes.

300 [Hz] the amplitude of  $y(t)$  at 4 [ $\mu$ s] is 0.309008 where as when  $m(t)$  operates at 500 [Hz] the amplitude at 4 [ $\mu$ s] is 0.308993. This is because there is a slower oscillation at 300 [Hz] and the amplitude is larger than the faster oscillations presented at 500 [Hz], see Fig 23. and 900 [Hz], see Fig. 24.

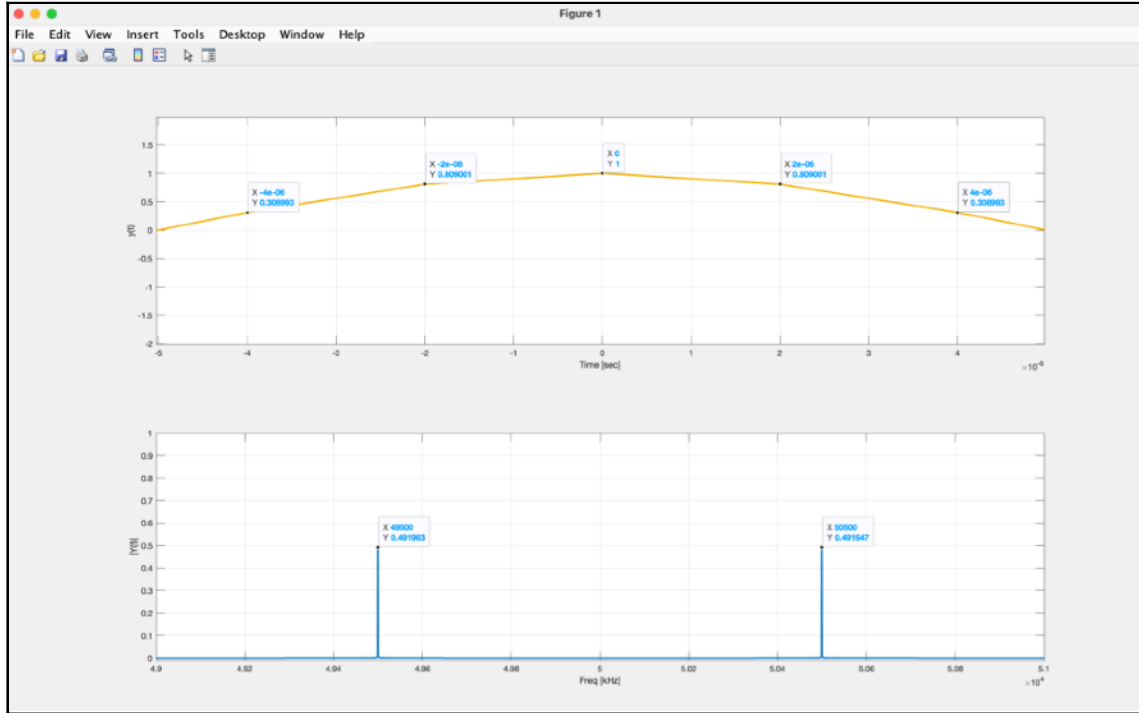


**Fig. 23** MATLAB plots from source code presented in **Fig. 21**. for  $m(t)$  with  $0.5$  [ $V_{p-p}$ ], frequency of  $500$  [Hz], and  $c(t)$  with  $2$  [ $V_{p-p}$ ] frequency of  $50$  [kHz]. The increase in oscillations from the  $300$  [Hz] to  $500$  [Hz] manifests as a larger frequency separation between the carrier frequency and the sidebands. Image © 2024 Yolanda Reyes.

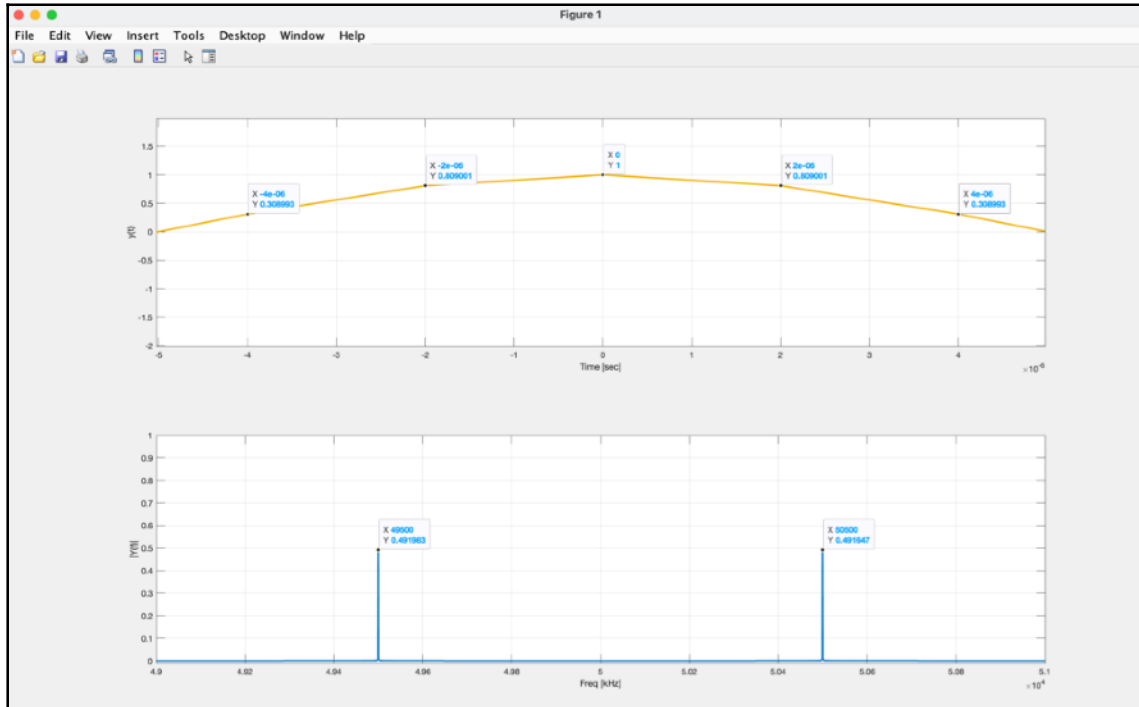


**Fig. 24** MATLAB plots from source code presented in **Fig. 21**. for  $m(t)$  with  $0.5$  [ $V_{p-p}$ ] frequency of  $900$  [Hz], and  $c(t)$  with  $2$  [ $V_{p-p}$ ] frequency of  $50$  [kHz]. The largest frequency separation between the carrier frequency and the sidebands was simulated with  $m(t)$  operating at  $900$  [Hz]. The Image © 2024 Yolanda Reyes.

The envelope of  $y(f)$  is determined by  $m(t)$  whose amplitude has not changed. However the spacing between peaks has decreased as  $m(t)$ 's frequency increases from 300 - 900 [Hz]. At 300 [Hz]  $m(t)$  has a period of 3.33 [ms], at 500 [Hz] the period is 2 [ms], and at 900 [Hz] the period is 1.11 [ms]. Visually we expect to see a visual “compression” of the signal since the envelope has not changed and there are more oscillations in the same amount of time.

### 3.2. LtSPICE

LtSPICE simulations to model the expected output voltages were created to give insight prior to the experiment portion of Lab 1. The LtSPICW simulations are a valuable tool when troubleshooting the experiment portion were implementation of the circuits presented in Fig. 4 - 6 is required. When issues are encountered with the physical circuit the simulation can be referenced to help diagnose where potential issues may be arising. For the plots presented in Fig. 25 - 27 the input voltage and output voltage across a load place holder resistor, see  $R_L$  in Fig. 5 & 6, are the only nodes of interest plotted.

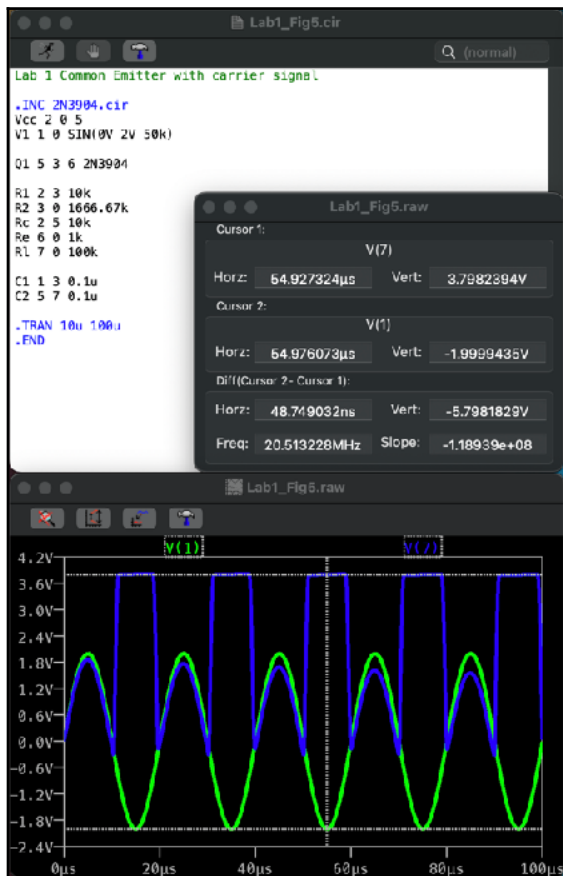


**Fig. 25** LtSPICE netlist for a common emitter NPN BJT configuration with carrier signal  $c(t)$  as  $V_1$ , in green, and  $V_{load}$ , in blue, plotted. Cursors are placed on both  $c(t)$  input  $V_1$  and output  $V_{load}$  which would be an antenna module in practice at  $\approx 55 \mu\text{s}$  to compare voltages at the same time. The Image © 2024 Yolanda Reyes.

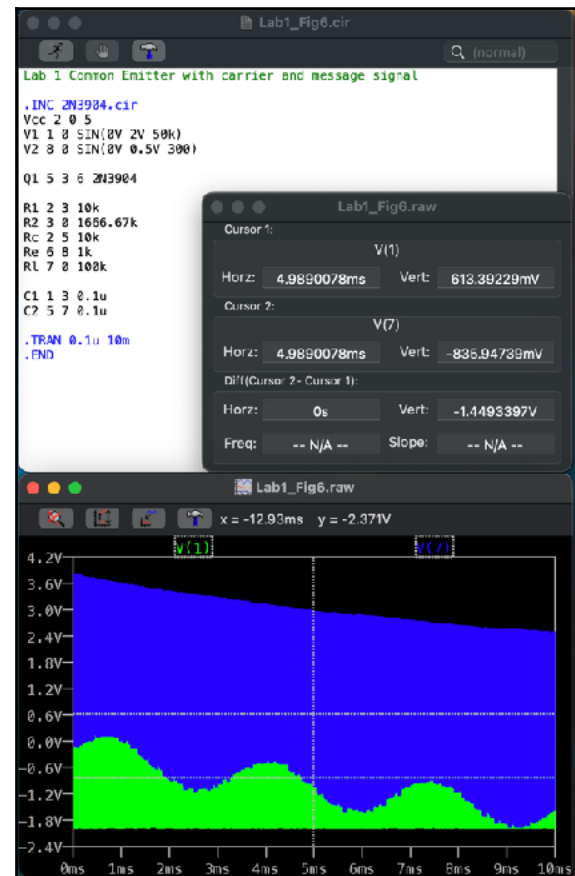


**Fig. 26** LtSPICE netlist for a common emitter NPN BJT configuration with carrier signal  $c(t)$  and message signal  $m(t)$ . The signal  $c(t)$  as  $V_1$ , in green, and  $V_{load}$ , in blue, are plotted. Cursors are placed on both  $c(t)$  input  $V_1$  and output  $V_{load}$  which would be an antenna module in practice at  $\approx 5 \text{ ms}$  to compare voltages at the same time. The Image © 2024 Yolanda Reyes.

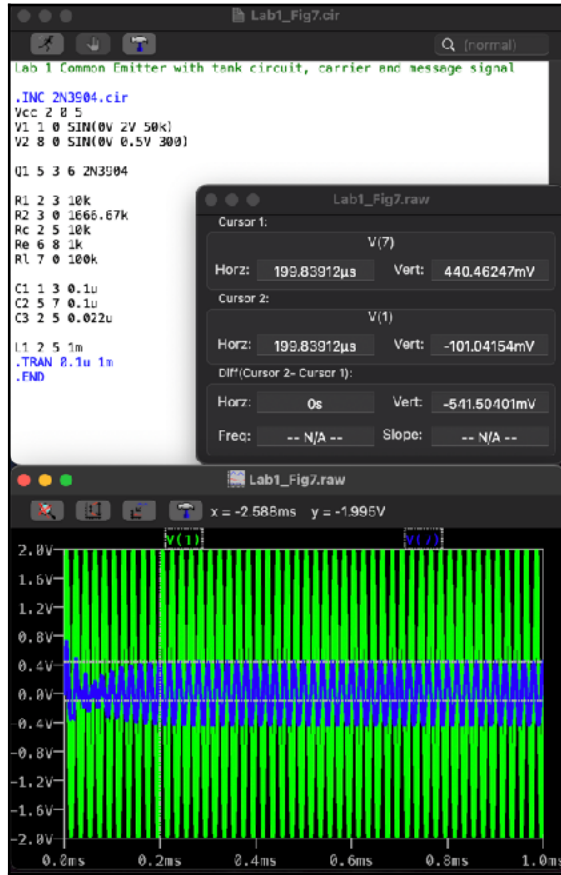


**Fig. 27** LtSPICE netlist for a common emitter NPN BJT configuration with carrier signal  $c(t)$ , message signal  $m(t)$  and tank circuit replacing  $R_c$  in **Fig. 6**. The signal  $c(t)$  as  $V_1$ , in green, and  $V_{load}$ , in blue, are plotted. Cursors are placed on both  $c(t)$  input  $V_1$  and output  $V_{load}$  which would be an antenna module in practice at  $\approx 200 \mu\text{s}$  to compare voltages at the same time. The Image © 2024 Yolanda Reyes.

## 4. Experimental Results

Using the Scopy platform for power supply, oscilloscope, and as signal generators for  $c(t)$  and  $m(t)$ , the setup for Lab 1 was implemented. The power supply provided power to  $V_{cc}$ , which enabled the voltage divider portion of the circuit design to provide sufficient turn on voltage to the base port of the NPN BJT  $Q_1$ , as well as voltage to the tank circuit when that portion was implemented. The signal generators provided our experimental signals to the circuit, see Fig. 28.

### 4.1. Common Emitter with Carrier Signal

The first step in implementing the AM transmitter circuit in Lab 1 is to construct a circuit using an NPN BJT transistor in the common emitter with emitter degeneration configuration which was presented in Fig. 6. With this first step implemented, see Fig. 29, we compare

the LtSPICE simulation results in Fig. 25 with oscilloscope output in Fig. 30 and determine the hardware is correctly implemented since the expected results match what was observed during the experiment in Lab 1.

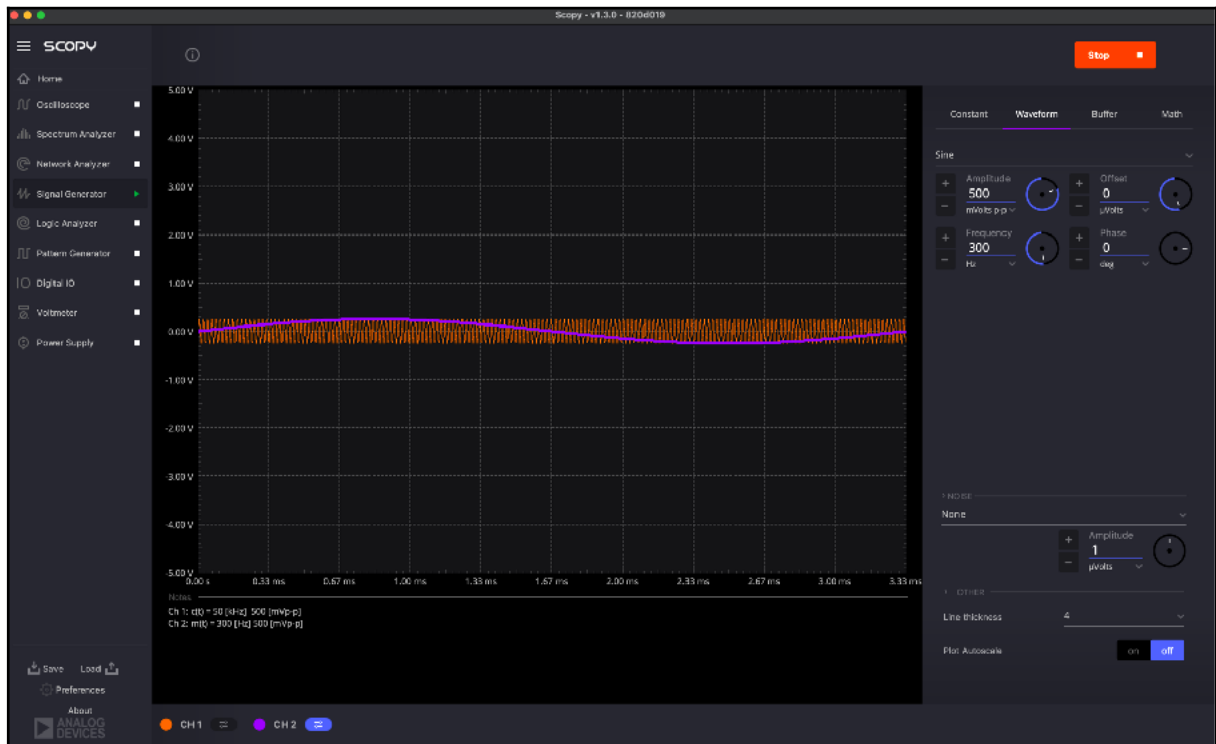


**Fig. 28** Scopy interface displaying carrier signal,  $c(t)$ , in orange on Channel 1, and message signal,  $m(t)$ , in purple on Channel 2. Both signals operate at 500 [mV<sub>p-p</sub>] Image © 2024 Yolanda Reyes.

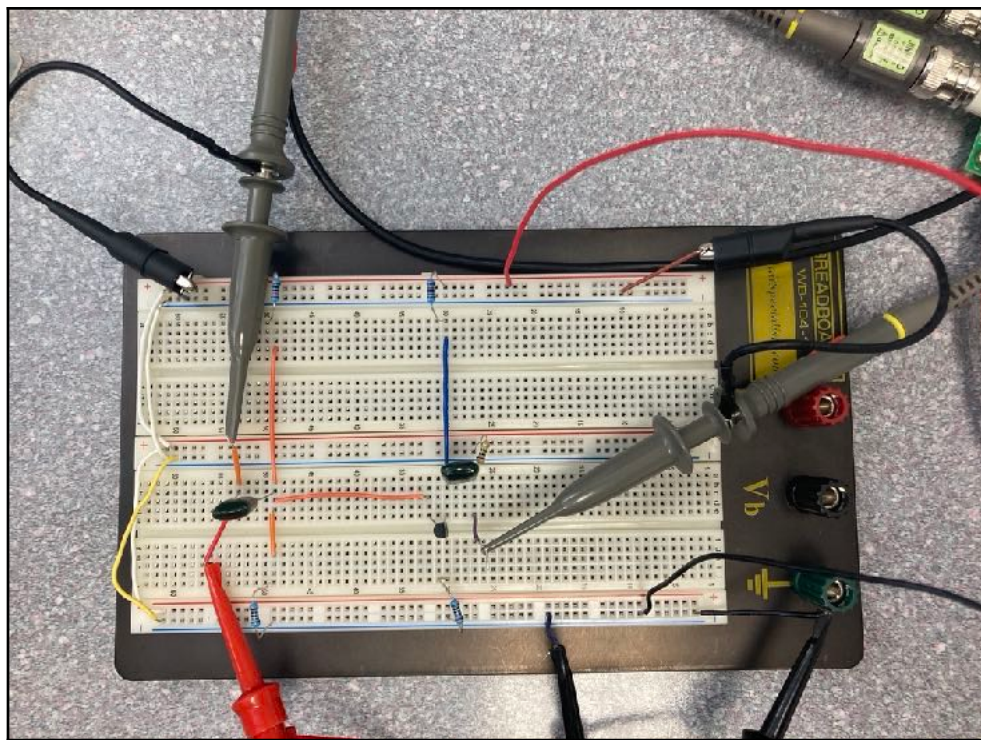


**Fig. 29** Common Emitter with emitter degeneration circuit presented in **Fig. 6**. Image © 2024 Yolanda Reyes.



**Fig. 30** Scopy plots with Channel 1 in orange demonstrating the carrier signal  $c(t)$ , and the expected output  $y(t)$  on Channel 2 in purple. These oscilloscope results match what was generated in LtSPICE simulations confirming the correct implementation in hardware of the circuit presented in Fig. 6. Image © 2024 Yolanda Reyes.

#### 4.2. Common Emitter with Carrier and Message Signal

With the first step completed correctly the next step in the experiment was to include the message signal,  $m(t)$ , into the design as presented in Fig. 31.

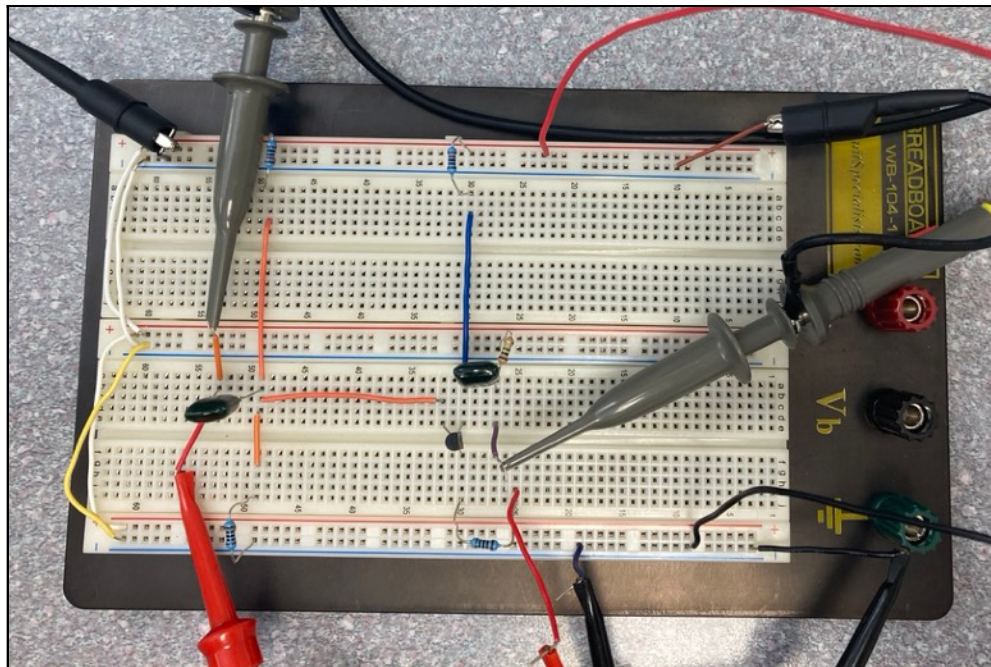


**Fig. 31** Common Emitter with emitter degeneration, carrier signal,  $c(t)$  on the left and message signal  $m(t)$  on the right. Image © 2024 Yolanda Reyes.

When comparing the output of the LtSPICE simulation previously performed for the common emitter with emitter degeneration,  $c(t)$ , and  $m(t)$  implementation, see Fig. 26., the experimental results of Lab 1, see Fig. 32., are confirmed to be correct.



**Fig. 32** Scopy plots with Channel 1 in orange demonstrating the carrier signal and the message signal on Channel 2 in purple. The frequency plot above the oscilloscope indicates that the operating frequency of the message signal is  $\approx 50$  [Hz]. Image © 2024 Yolanda Reyes.

#### 4.3. Common Emitter with Message Signals and Tank Circuit

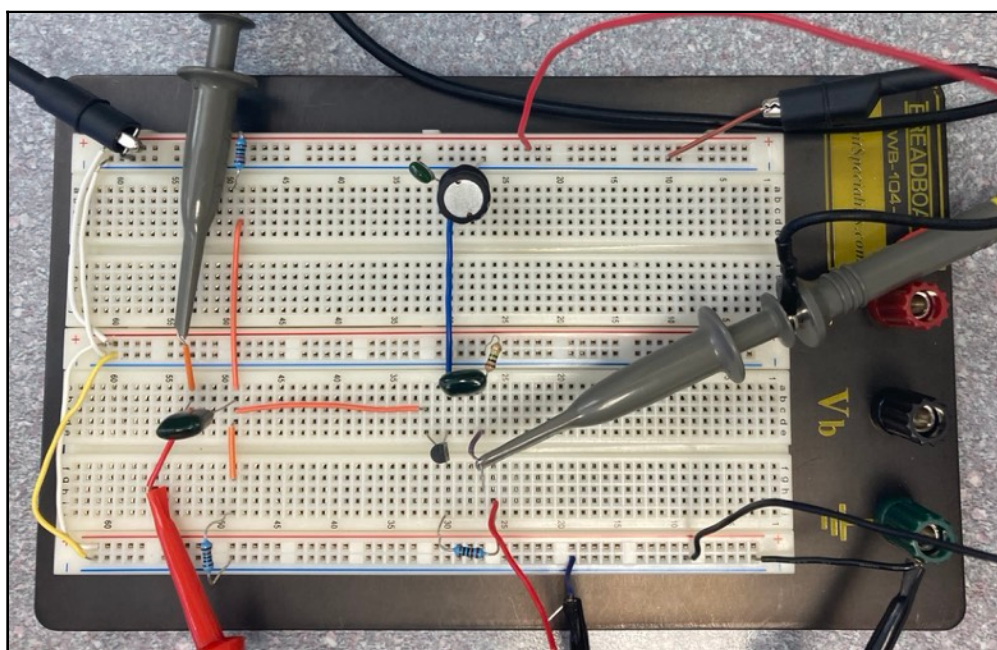


**Fig. 33** Common Emitter with emitter degeneration, carrier signal,  $c(t)$  on the left, message signal  $m(t)$  on the right and tank circuit with  $C_3 = 0.01$  [ $\mu$ F] and  $L_3 = 1$  [mH] as presented in Fig. 5. Image © 2024 Yolanda Reyes.

The next step in Lab 1 was to implement, see Fig. 33., the tank circuit initially presented in Fig. 5 using initial value of  $0.01 \mu\text{F}$  for  $C_3$ . When comparing the output of the LtSPICE simulation previously performed for the common emitter with emitter degeneration,  $c(t)$ ,  $m(t)$ , and tank circuit implementation, see Fig. 27., the experimental results of Lab 1, see Fig. 34., are confirmed to be correct.



**Fig. 34** Scopy plots with the message signal on Channel 2 in purple. The frequency plot above the oscilloscope indicates that the operating frequency of the message signal with the tank circuit implemented is  $\approx 2.50 \text{ [kHz]}$ . The top image showcases a voltage of  $298.077 \text{ [mV]}$  which is considered to be this system's logic high, or binary 1 in our modulated output signal  $y(t)$ . The bottom image showcases a voltage of  $50.481 \text{ [mV]}$  which is considered to be this system's logic low, or binary 0 in our modulated output signal  $y(t)$ . Image © 2024 Yolanda Reyes.

#### 4.4. Tank Circuit Tuning with Capacitors

The last step in Lab 1 was to switch out  $C_3$  capacitors to vary the tank circuit's resonance frequency and observe the results. The two capacitors I choose to observe had values of 0.022 [ $\mu\text{F}$ ], see Fig. 35 & 37., and 0.047 [ $\mu\text{F}$ ], see Fig. 36 & 38.

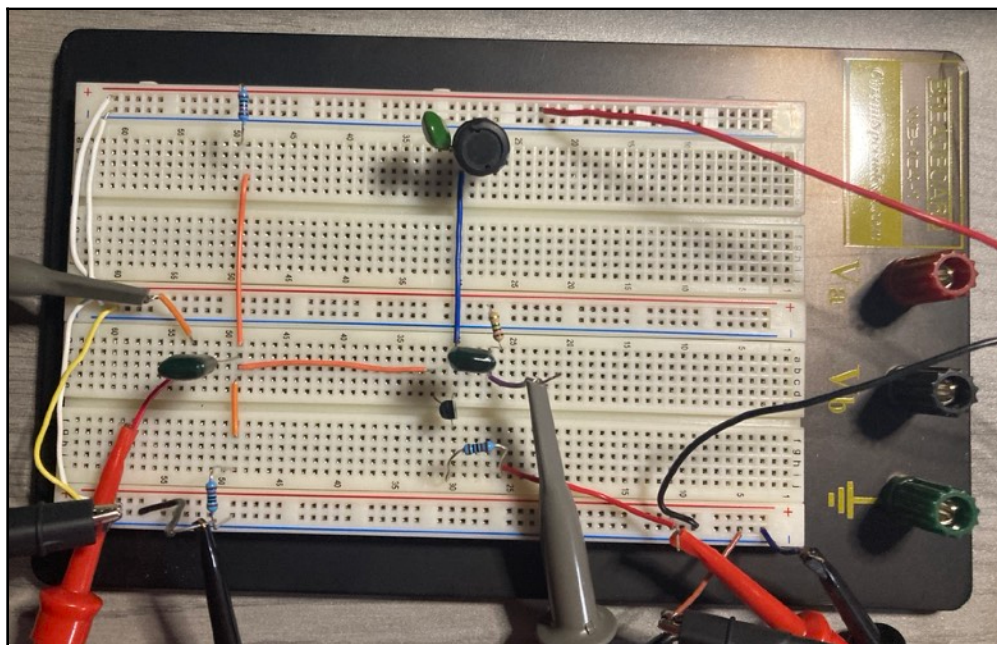


Fig. 35 Common Emitter with emitter degeneration, carrier signal,  $c(t)$  on the left, message signal  $m(t)$  on the right and tank circuit with  $C_3 = 0.022\text{ }\mu\text{F}$  and  $L_3 = [1\text{mH}]$  as presented in Fig. 5. Image © 2024 Yolanda Reyes.

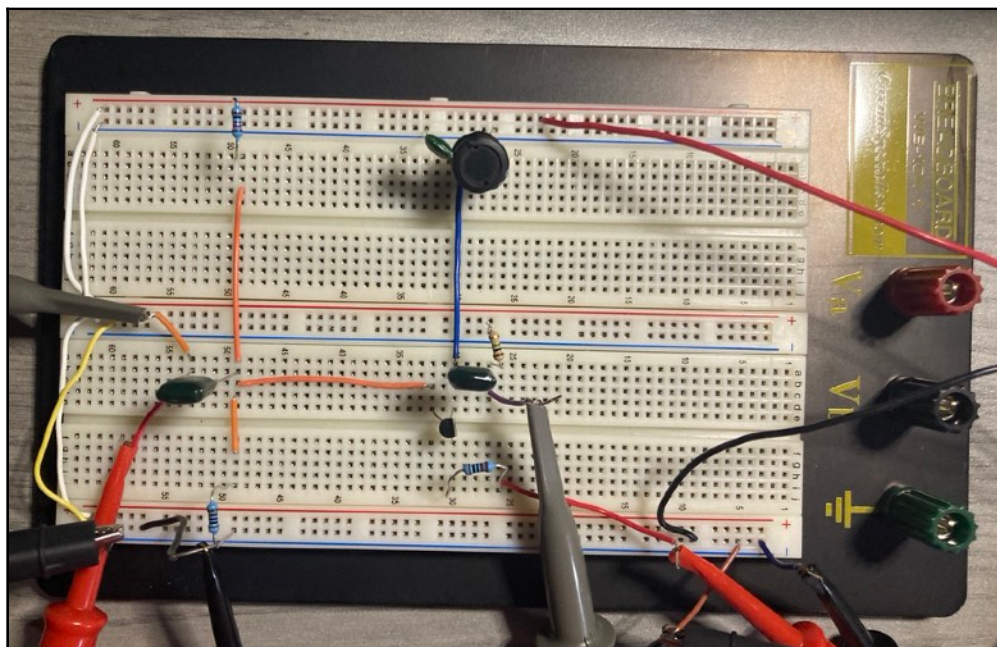
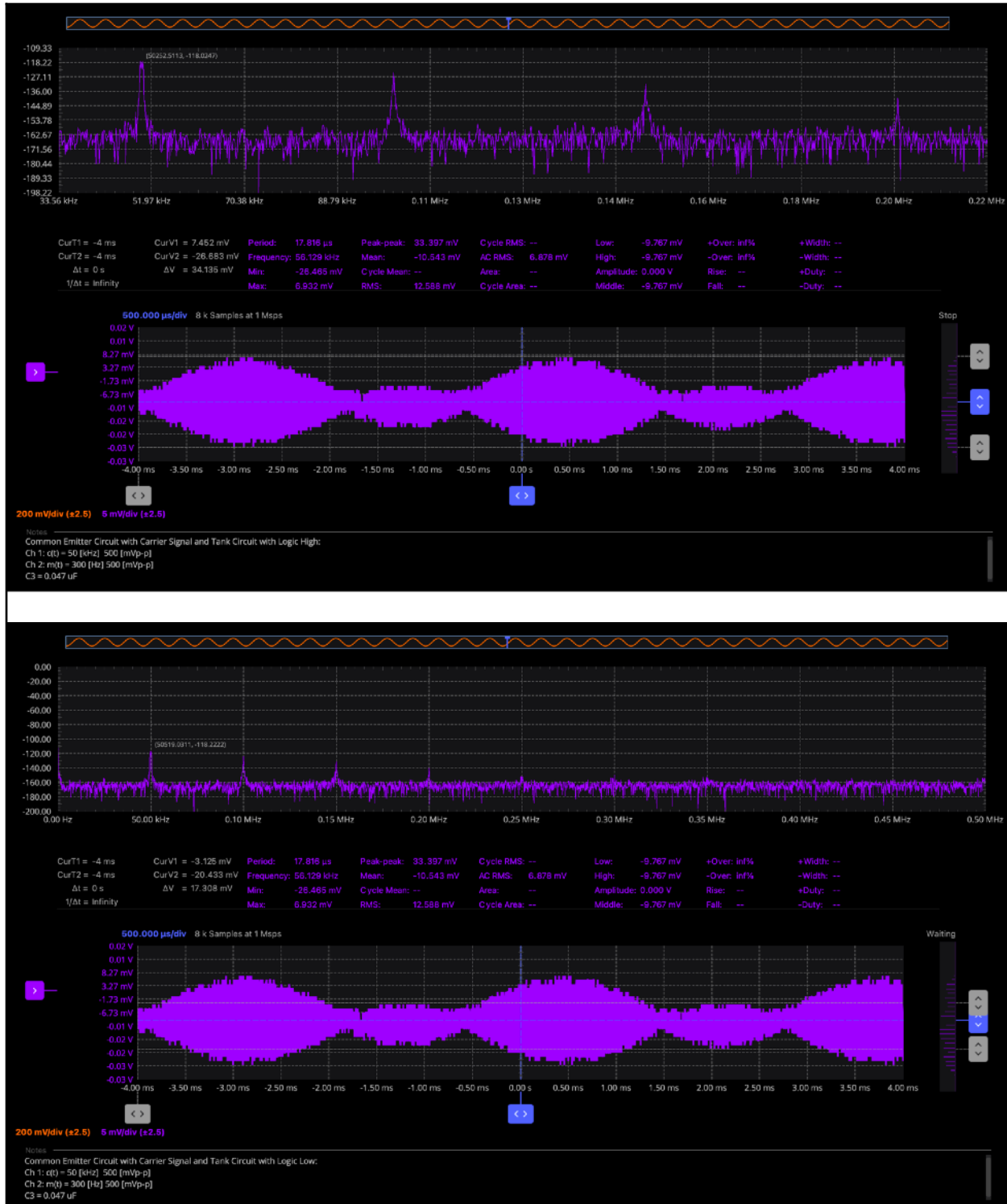


Fig. 36 Common Emitter with emitter degeneration, carrier signal,  $c(t)$  on the left, message signal  $m(t)$  on the right and tank circuit with  $C_3 = 0.047\text{ }\mu\text{F}$  and  $L_3 = [1\text{mH}]$  as presented in Fig. 5. Image © 2024 Yolanda Reyes.



**Fig. 37** Common Emitter with emitter degeneration, carrier signal,  $c(t)$  on the left, message signal  $m(t)$  on the right and tank circuit with  $C_3 = 0.022$  [ $\mu$ F] and  $L_3 = [1mH]$  as presented in Fig. 35. For this implementation of the AM transmitter circuit logic high/binary 1 is measured to be 84.615 [mV], were as logic low/binary 0 is measured to be 40.865 [mV]. Image © 2024 Yolanda Reyes.



**Fig. 38** Common Emitter with emitter degeneration, carrier signal,  $c(t)$  on the left, message signal  $m(t)$  on the right and tank circuit with  $C_3 = 0.047 \mu\text{F}$  and  $L_3 = [1\text{mH}]$  as presented in **Fig. 36**. For this implementation of the AM transmitter circuit logic high/binary 1 is measured to be 34.135 [mV], were as logic low/binary 0 is measured to be 17.308 [mV]. Image © 2024 Yolanda Reyes.

The circuit designed for Lab 1 uses the Amplitude Modulation (AM) scheme for RF communication and the tank circuit directly affects the amplitude and bandwidth of the

output signal  $y(t)$ . If the tank circuit is not tuned to resonate close to the carrier signal  $c(t)$ , 50 [kHz] in the case of Lab 1, then performance will not be optimal. Referring to calculations presented in the theoretical calculation portion of this report, Fig. 19, we expect the tank circuit using  $C_3=0.022 \text{ } [\mu\text{F}]$  to resonate at 1.073 [kHz], which is significantly lower than the carrier signal  $c(t)$ , see Fig. 38. When we implement the same design, see Fig. 39., using  $C_3=0.047 \text{ } [\mu\text{F}]$  instead the resonating frequency of the tank circuit becomes 734.127 [Hz], even lower than the carrier signal.

Adjusting the values of  $C_3$  will enable the design to be tuned to enhance bandwidth or gain at specific frequencies but can also lead to less optimal signal generation prior to transmission and reduce circuit efficiency. By increasing  $C_3$  we decrease the Q-factor which leads to a broader bandwidth making the circuit less capable of being selective when filtering out frequencies around the resonance frequency.

## 5. Results and Conclusion

### 5.1. Results

For Lab 1 three AM transmitter circuits were designed with varying features as showcased in Table 1. Only one of the circuits optimized the transmitter output to the next module which would traditionally be an amplifier or antenna circuit.

Table 1

| Tank Circuit<br>$C_3 \text{ } [\mu\text{F}]$ | Carrier Signal:<br>$c(t) \text{ } [\text{kHz}]$ | Message Signal:<br>$m(t) \text{ } [\text{Hz}]$ | Modulated Signal:<br>$y(t) \text{ } [\text{kHz}]$ | Binary "0" [mV] | Binary "1" [mV] | Modulation Index                     |
|----------------------------------------------|-------------------------------------------------|------------------------------------------------|---------------------------------------------------|-----------------|-----------------|--------------------------------------|
| 0.01                                         | 50                                              | 300                                            | 2.5                                               | 50.481          | 298.077         | 0.3% Logic High<br>0.51% Logic Low   |
| 0.022                                        | 50                                              | 300                                            | 250                                               | 40.865          | 84.615          | 0.09% Logic High<br>0.041% Logic Low |
| 0.047                                        | 50                                              | 300                                            | 50.25                                             | 17.308          | 34.135          | 0.034% Logic High<br>1.73% Logic Low |

### 5.2. Discussion

Starting with the calculations of the Lab 1 work obstacles I encountered included calculating the NPN BJT in saturation mode initially, see Fig. 8 - 10., I did not realize before the deadline for the homework submission that I needed to change the value of  $R_2$  so that the voltage divider portion of the circuit would send enough voltage to the base port of the transistor. By the time I went to the lab and performed the experiment I still had not calculated the value of  $R_2$  and therefore performed the experiment with the suggested value of 1 [ $\text{k}\Omega$ ]. After the experiment was performed I was able to calculate, see Fig. 11, a value for  $R_2$  of 2 [ $\text{k}\Omega$ ]. If I was able to perform the experiment again I would utilize a resistor as close to the value of 2 [ $\text{k}\Omega$ ] as possible and compare the results from the first and update Table 1 accordingly.

The calculations for the modulation index are not what I expected when implementing the experiment with a capacitor  $C_3$  value of 0.01 [ $\mu\text{F}$ ]. According to calculations the tank circuit implementation with  $C_3$  at this value should optimize the circuits ability to transmit the modulated signal since the tank circuit is resonating close to 50 [kHz], which is the frequency of our carrier signal. However the values presented in Fig. 34 indicate that the modulated signal is operating at 2.5 [kHz]. In an ideal setting, which our experiment was not due to real world limitations, I would assume the modulated signal would operate close to the carrier frequency. I was surprised that it was oscillating at a frequency that was significantly lower than the carrier frequency. Some hypothesis developed to explain this discrepancy in the data include:

1. Lack of calibration of the Scopy module prior to running the experiment. Prior use of the ADALM 2000 module didn't require calibration before every experiment so this step was not part of my usual workflow.
2. Ambiguity of the Scopy interface, some students did not have x-axis values present during the experiment and perhaps the values aren't correct due to what ever bug was present in the software that removed the frequency labels for my peers.
3. This was the first lab that required the use of a spectrum analyzer, therefore I had no prior experience using this diagnostic tool. Perhaps the FFT plot in Fig. 34 indicates an offset of 2.5 [kHz] I am not sure since I have only used this tool once.
4. Dr. Lee mentioned in lecture that there are limitations to what we can actually experiment due to the hardware we have available. Perhaps these limitations are giving me such a different value then I expected.

During the LtSPICE simulations I ran into considerable trouble trying to view the voltage plots for the carrier signal  $c(t)$ , message signal  $m(t)$ , and modulated signal  $y(t)$ . I am still developing a workflow for knowing what the settings using the .TRAN operation in LtSPICE should be. After the homework was submitted and example plots were released I was able to implement the same settings however my plots for circuit 2 and circuit 3 do not look like what was provided as examples of what we should get. In the experiment my oscilloscope traces resemble what was provided in Canvas but I am still not sure why my LtSPICE plots do not look like what I expect. Some hypothesis developed to explain this discrepancy in my simulation plots verse my experimental data include:

1. I am still not using good values for the .TRAN operation to accurately reflect what I got in the experiment, or what Dr. Lee provided as example output on Canvas. Although I am using the same values based on the examples provided so this is not a solid hypothesis to explain the plot discrepancies.

2. The last LtSPICE simulations I ran I put R<sub>2</sub> as 1666.67 [kΩ], however during the writing of this report I realized/remembered that this resistor should be 2 [kΩ], and that the value I simulated was the Thevenin resistance I calculated. If there was more time I would re-run the simulation, and update this document.

Another obstacle I ran into when attempting to perform the LtSPICE simulations for the homework submission was that I forgot to add the V<sub>cc</sub> power supply so all my plots for the homework submission were returning voltages of 0 [V]. After the experiment I was able to get feedback and fixed this issue for this report.

The experiment portion of this lab presented a few questions mainly revolving around the calculation of the modulation index and the discrepancies in spectrum analyzer. Perhaps the resistors not being the exact values used in theoretical calculations and simulations had an impact on my final results. I would not expect the values for this data to vary too much since the values of the components were assumed to be in an acceptable range to match with calculations and simulations:

$$\begin{aligned}R_1 &= 9.95 \text{ [k}\Omega\text{]} \\R_2 &= 0.996 \text{ [k}\Omega\text{]} \\R_C &= 9.97 \text{ [k}\Omega\text{]} \\R_E &= 0.998 \text{ [k}\Omega\text{]} \\R_L &= 1005 \text{ [k}\Omega\text{]}\end{aligned}$$

### 5.3. Conclusion

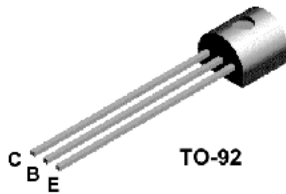
In Lab 1 we implemented a simple amplitude modulation (AM) modulator for a radio frequency (RF) transmitter. By using an NPN BJT in common emitter configuration with emitter degeneration and a tank circuit we can observe a modulated signal that would in practice be sent to an antenna for transmission. Due to legal and discrete component limitations we were not able to replicate the system that was presented in lecture but were able to observe the fundamentals behind the components and transmitter module present in SDR applications. By implementing a tank circuit with different capacitor values we are able to observe different tuning abilities and how the resonate frequency of this portion of the circuit affects the modulated signal's quality. Ideally the tank circuit should resonate as close to the carrier frequency, in this case 50 [kHz], so that the transmitter doesn't attenuate the carrier frequency. The message signal modulates this carrier signal using amplitude modulation and will be present in the side lobes in the spectrum analyzer at around 49.7 [kHz] and 50.3 [kHz]. According to the calculations performed for the MATLAB simulations we should see a modulation index value of 25%.

## 6. Datasheet: 2N3904 NPN BJT

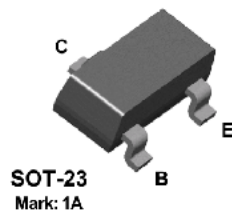
ՆԱԽԵՆ / ԲԱՐՁՐ / ՀԱՅՐԱՎ / ՀԱՅՐԱՎ



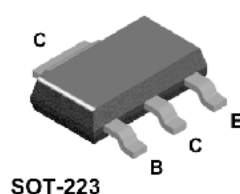
**2N3904**



**MMBT3904**



**PZT3904**



### NPN General Purpose Amplifier

This device is designed as a general purpose amplifier and switch. The useful dynamic range extends to 100 mA as a switch and to 100 MHz as an amplifier.

#### Absolute Maximum Ratings\*

$T_A = 25^\circ\text{C}$  unless otherwise noted

| Symbol         | Parameter                                        | Value       | Units            |
|----------------|--------------------------------------------------|-------------|------------------|
| $V_{CEO}$      | Collector-Emitter Voltage                        | 40          | V                |
| $V_{CBO}$      | Collector-Base Voltage                           | 60          | V                |
| $V_{EBO}$      | Emitter-Base Voltage                             | 6.0         | V                |
| $I_C$          | Collector Current - Continuous                   | 200         | mA               |
| $T_J, T_{Stg}$ | Operating and Storage Junction Temperature Range | -55 to +150 | $^\circ\text{C}$ |

\*These ratings are limiting values above which the serviceability of any semiconductor device may be impaired.

**NOTES:**

- 1) These ratings are based on a maximum junction temperature of 150 degrees C.
- 2) These are steady state limits. The factory should be consulted on applications involving pulsed or low duty cycle operations.

#### Thermal Characteristics

$T_A = 25^\circ\text{C}$  unless otherwise noted

| Symbol    | Characteristic                                | Max        |            |              | Units                      |
|-----------|-----------------------------------------------|------------|------------|--------------|----------------------------|
|           |                                               | 2N3904     | *MMBT3904  | **PZT3904    |                            |
| $P_D$     | Total Device Dissipation<br>Derate above 25°C | 625<br>5.0 | 350<br>2.8 | 1,000<br>8.0 | mW<br>mW/ $^\circ\text{C}$ |
| $R_{HJC}$ | Thermal Resistance, Junction to Case          | 83.3       |            |              | $^\circ\text{C/W}$         |
| $R_{HJA}$ | Thermal Resistance, Junction to Ambient       | 200        | 357        | 125          | $^\circ\text{C/W}$         |

\*Device mounted on FR-4 PCB 1.6" X 1.6" X 0.06."

\*\*Device mounted on FR-4 PCB 36 mm X 18 mm X 1.5 mm; mounting pad for the collector lead min. 6 cm<sup>2</sup>.

## NPN General Purpose Amplifier

(continued)

### Electrical Characteristics

$T_A = 25^\circ\text{C}$  unless otherwise noted

| Symbol | Parameter | Test Conditions | Min | Max | Units |
|--------|-----------|-----------------|-----|-----|-------|
|--------|-----------|-----------------|-----|-----|-------|

#### OFF CHARACTERISTICS

|                             |                                     |                                             |     |    |    |
|-----------------------------|-------------------------------------|---------------------------------------------|-----|----|----|
| $V_{(\text{BR})\text{CEO}}$ | Collector-Emitter Breakdown Voltage | $I_C = 1.0 \text{ mA}, I_B = 0$             | 40  |    | V  |
| $V_{(\text{BR})\text{CBO}}$ | Collector-Base Breakdown Voltage    | $I_C = 10 \mu\text{A}, I_E = 0$             | 60  |    | V  |
| $V_{(\text{BR})\text{EBO}}$ | Emitter-Base Breakdown Voltage      | $I_E = 10 \mu\text{A}, I_C = 0$             | 6.0 |    | V  |
| $I_{BL}$                    | Base Cutoff Current                 | $V_{CE} = 30 \text{ V}, V_{EB} = 3\text{V}$ |     | 50 | nA |
| $I_{CEX}$                   | Collector Cutoff Current            | $V_{CE} = 30 \text{ V}, V_{EB} = 3\text{V}$ |     | 50 | nA |

#### ON CHARACTERISTICS\*

|                      |                                      |                                                                                            |      |              |        |
|----------------------|--------------------------------------|--------------------------------------------------------------------------------------------|------|--------------|--------|
| $h_{FE}$             | DC Current Gain                      | $I_C = 0.1 \text{ mA}, V_{CE} = 1.0 \text{ V}$                                             | 40   |              |        |
|                      |                                      | $I_C = 1.0 \text{ mA}, V_{CE} = 1.0 \text{ V}$                                             | 70   |              |        |
|                      |                                      | $I_C = 10 \text{ mA}, V_{CE} = 1.0 \text{ V}$                                              | 100  |              |        |
|                      |                                      | $I_C = 50 \text{ mA}, V_{CE} = 1.0 \text{ V}$                                              | 60   | 300          |        |
|                      |                                      | $I_C = 100 \text{ mA}, V_{CE} = 1.0 \text{ V}$                                             | 30   |              |        |
| $V_{CE(\text{sat})}$ | Collector-Emitter Saturation Voltage | $I_C = 10 \text{ mA}, I_B = 1.0 \text{ mA}$<br>$I_C = 50 \text{ mA}, I_B = 5.0 \text{ mA}$ |      | 0.2<br>0.3   | V<br>V |
| $V_{BE(\text{sat})}$ | Base-Emitter Saturation Voltage      | $I_C = 10 \text{ mA}, I_B = 1.0 \text{ mA}$<br>$I_C = 50 \text{ mA}, I_B = 5.0 \text{ mA}$ | 0.65 | 0.85<br>0.95 | V<br>V |

#### SMALL SIGNAL CHARACTERISTICS

|           |                                  |                                                                                                                   |     |     |     |
|-----------|----------------------------------|-------------------------------------------------------------------------------------------------------------------|-----|-----|-----|
| $f_T$     | Current Gain - Bandwidth Product | $I_C = 10 \text{ mA}, V_{CE} = 20 \text{ V}, f = 100 \text{ MHz}$                                                 | 300 |     | MHz |
| $C_{obo}$ | Output Capacitance               | $V_{CB} = 5.0 \text{ V}, I_E = 0, f = 1.0 \text{ MHz}$                                                            |     | 4.0 | pF  |
| $C_{ibo}$ | Input Capacitance                | $V_{EB} = 0.5 \text{ V}, I_C = 0, f = 1.0 \text{ MHz}$                                                            |     | 8.0 | pF  |
| NF        | Noise Figure                     | $I_C = 100 \mu\text{A}, V_{CE} = 5.0 \text{ V}, R_S = 1.0 \text{k}\Omega, f = 10 \text{ Hz to } 15.7 \text{ kHz}$ |     | 5.0 | dB  |

#### SWITCHING CHARACTERISTICS

|       |              |                                                                                                |  |     |    |
|-------|--------------|------------------------------------------------------------------------------------------------|--|-----|----|
| $t_d$ | Delay Time   | $V_{CC} = 3.0 \text{ V}, V_{BE} = 0.5 \text{ V}, I_C = 10 \text{ mA}, I_{B1} = 1.0 \text{ mA}$ |  | 35  | ns |
| $t_r$ | Rise Time    |                                                                                                |  | 35  | ns |
| $t_s$ | Storage Time | $V_{CC} = 3.0 \text{ V}, I_C = 10 \text{ mA}$                                                  |  | 200 | ns |
| $t_f$ | Fall Time    | $I_{B1} = I_{B2} = 1.0 \text{ mA}$                                                             |  | 50  | ns |

\*Pulse Test: Pulse Width  $\leq 300 \mu\text{s}$ , Duty Cycle  $\leq 2.0\%$

#### Spice Model

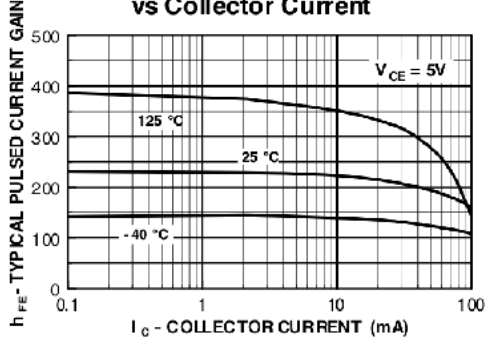
NPN (Is=6.734f Xti=3 Eg=1.11 Vaf=74.03 Bf=416.4 Ne=1.259 Ise=6.734 Ikf=66.78m Xtb=1.5 Br=.7371 Nc=2 Isc=0 Ikr=0 Rc=1 Cjc=3.638p Mjc=.3085 Vjc=.75 Fc=.5 Cje=4.493p Mje=.2593 Vje=.75 Tr=239.5n Tf=301.2p If=.4 Vtf=4 Xtf=2 Rb=10)

## NPN General Purpose Amplifier

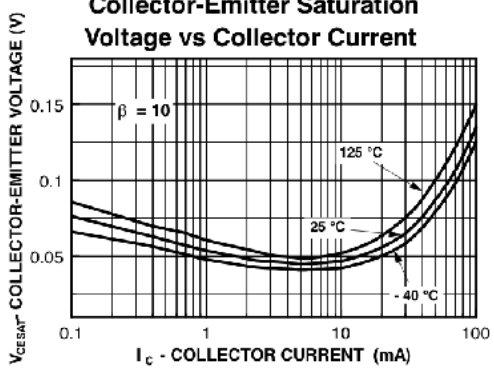
(continued)

### Typical Characteristics

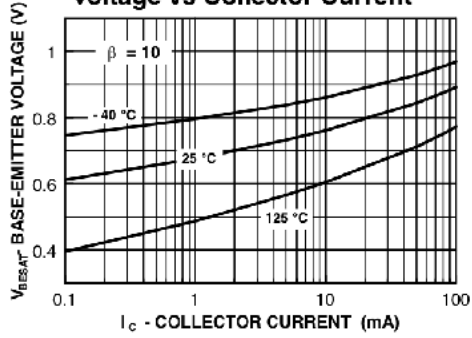
**Typical Pulsed Current Gain vs Collector Current**



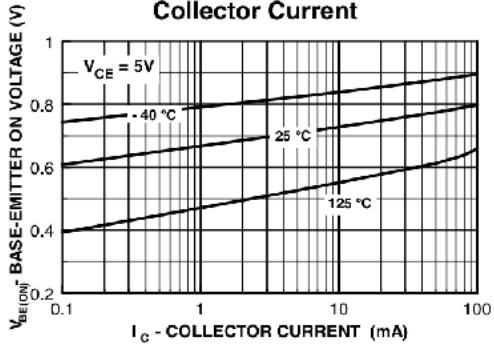
**Collector-Emitter Saturation Voltage vs Collector Current**



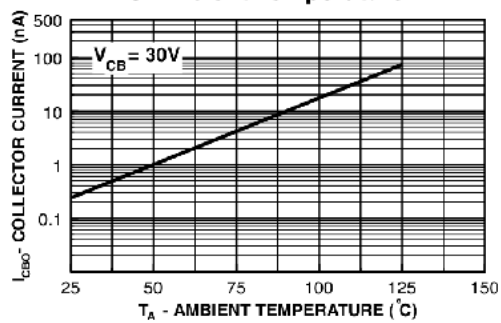
**Base-Emitter Saturation Voltage vs Collector Current**



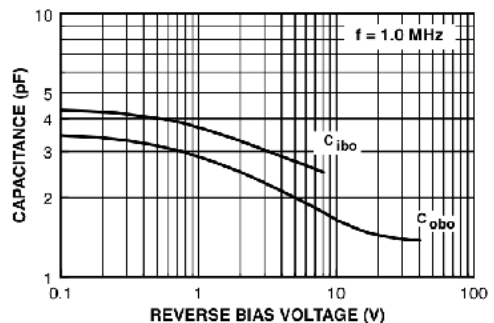
**Base-Emitter ON Voltage vs Collector Current**



**Collector-Cutoff Current vs Ambient Temperature**



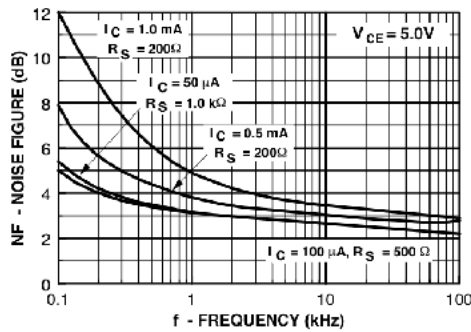
**Capacitance vs Reverse Bias Voltage**



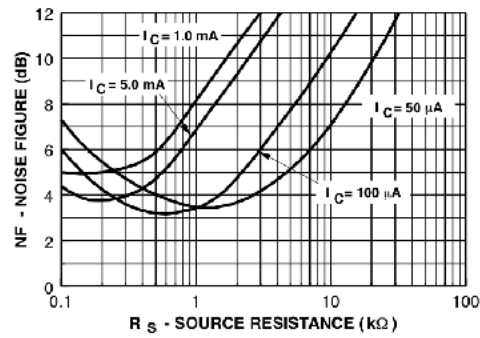
**NPN General Purpose Amplifier**  
(continued)

**Typical Characteristics** (continued)

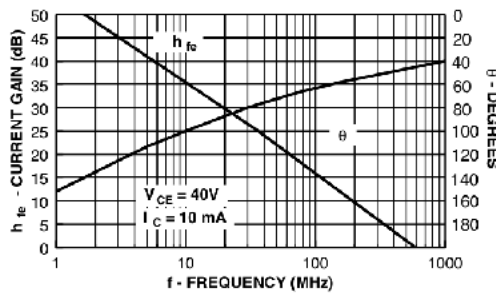
**Noise Figure vs Frequency**



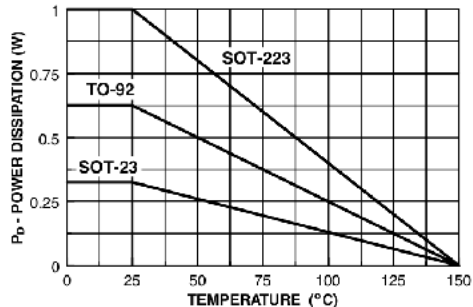
**Noise Figure vs Source Resistance**



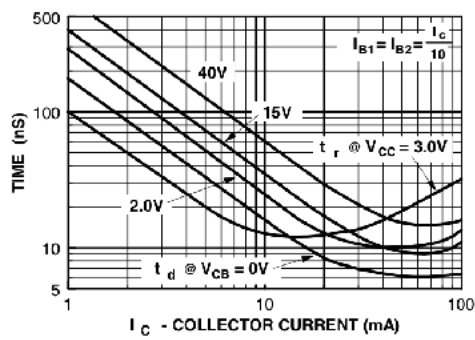
**Current Gain and Phase Angle vs Frequency**



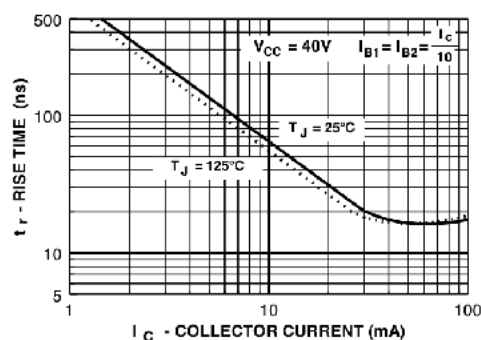
**Power Dissipation vs Ambient Temperature**



**Turn-On Time vs Collector Current**



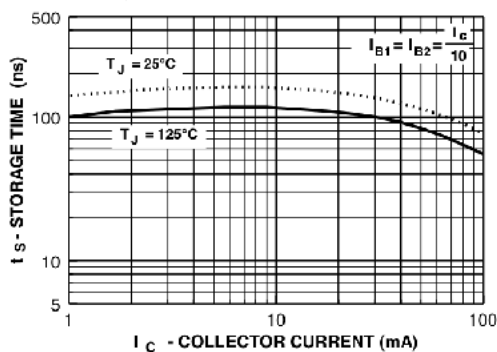
**Rise Time vs Collector Current**



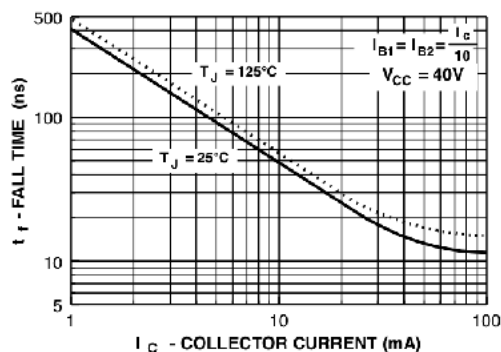
**NPN General Purpose Amplifier**  
(continued)

**Typical Characteristics** (continued)

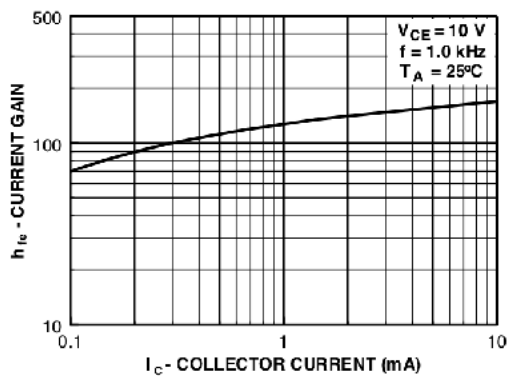
**Storage Time vs Collector Current**



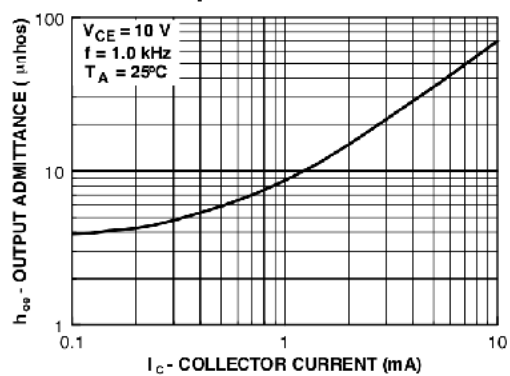
**Fall Time vs Collector Current**



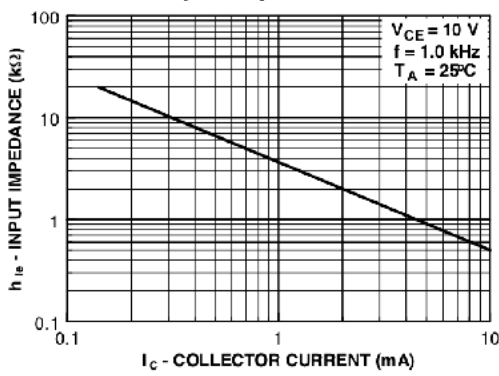
**Current Gain**



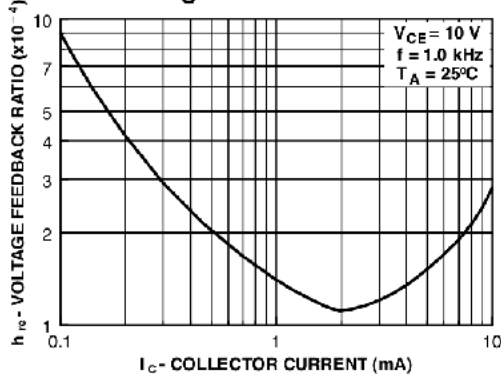
**Output Admittance**



**Input Impedance**



**Voltage Feedback Ratio**



**NPN General Purpose Amplifier**  
(continued)

**Test Circuits**

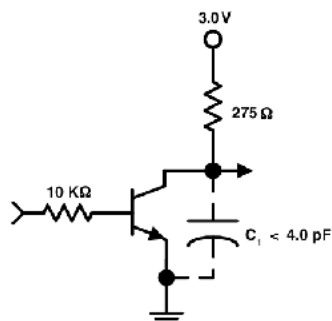
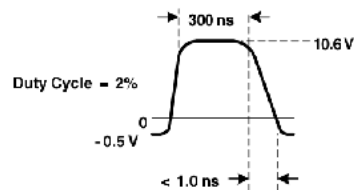


**FIGURE 1: Delay and Rise Time Equivalent Test Circuit**

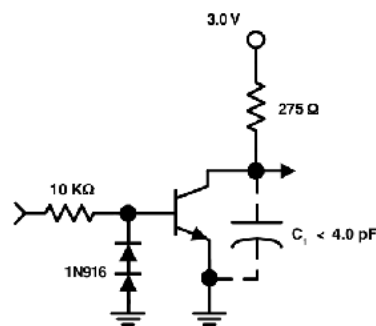
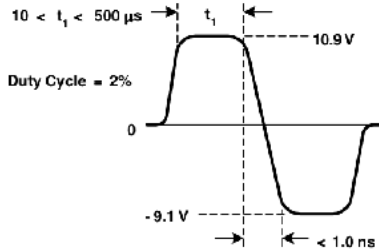


**FIGURE 2: Storage and Fall Time Equivalent Test Circuit**

## 7. References

- [1] Heilbron, J. L. (ed.), "The Oxford Guide to the History of Physics and Astronomy", Oxford, UK: Oxford University Press, 2005, pp. 148.
- [2] T. White, "United States Early Radio History," *Word Origins-Radio*, section 22. Accessed: Sept. 18, 2024. [Online]. Available: <https://earlyradiohistory.us/sec022.htm.\>
- [3] Belrose, J., "Marconi and the History of Radio," *IEEE Antennas and Propagation Magazine*, Vol. 46, No. 2, 2004, pp.130
- [4] International Telecommunications Union, G.711: Pulse Code Modulation (PCM) of Voice Frequencies. Accessed: Sept. 18, 2024. [Online]. Available: <http://www.itu.int/rec/T-REC-G.711/>
- [5] Hauben, R., "From the ARPANET to the Internet," *TCP Digest(UUCP)*, January 2001. Accessed: Sept. 18, 2024. [Online]. Available: [http://www.columbia.edu/~rh120/other/tcpdigest\\_paper.txt](http://www.columbia.edu/~rh120/other/tcpdigest_paper.txt)
- [6] International Telecommunications Union, G.722: 7 kHz Audio-Coding within 64 kbit/s, Accessed: Sept. 18, 2024. [Online]. Available: <https://www.itu.int/rec/T-REC-G.722>
- [7] Kilby, J., *Miniatrized Electronic Circuits*, 1964, US Patent No. 3,138,743. Accessed: Sept. 18, 2024. [Online]. Available: <https://www.google.com/patents/US3138743>
- [8] Moore, G., Lithography and the Future of Moore's Law," *SPIE*, Vol.2438, 1995. Accessed: Sept. 18, 2024. [Online]. Available: <http://www.lithoguru.com/scientist/CHE323/Moore1995.pdf>
- [9] Kester, W., *The Data Conversion Handbook*, Analog Devices, 2005. Accessed: Sept. 18, 2024. [Online]. Available: <http://www.analog.com/en/education/education-library/data-conversion-handbook.html>
- [10] Hall, B., and W. Taylor, "X- and Ju-Band Samll Form Factor Radio Design," Analog Devices Inc., Wilmington, MA, 2017. Accessed: Sept. 18, 2024. [Online]. Available: <http://www.analog.com/en/technical-articles/x-and-ku-band-small-form-factor-radio-design.html>
- [11] Pickle, B. "Modulation", Sharpened Productions, Accessed: Sept. 18, 2024. [Online]. Available: <https://techterms.com/definition/modulation>

- [12] H. Kwasme and S. Ekin, "RSSI-Based Localization Using LoRaWAN Technology," IEEE Access, vol. 7, pp. 99856-99866, 2019. Accessed: Sept. 18, 2024. [Online]. Available: <https://ieeexplore.ieee.org/document/8764340>